Summer 6-4-2021

Modeling Evolution of Intratumor Phenotypic Heterogeneity in Metastasis and Cancer Drug Resistance

Bin Zhang

Recommended Citation
Zhang, Bin, "Modeling Evolution of Intratumor Phenotypic Heterogeneity in Metastasis and Cancer Drug Resistance." Dissertation, Georgia State University, 2021.
doi: https://doi.org/10.57709/23193070

Modeling Evolution of Intratumor Phenotypic Heterogeneity in Metastasis and Cancer Drug Resistance

by

Bin Zhang

Under the Direction of Yi Jiang, PhD

ABSTRACT

Most tumors are complex ecosystems that emerge and evolve under robust selective pressure from their microenvironment. Such a pressure promotes the diversification of both tumor cells and the tumor microenvironment, resulting in increased intratumoral heterogeneity (ITH) that enables aggressive disease progression leading to metastasis and resistance to treatment. Metastasis and the emergence of chemo-resistance are the two main reasons for cancer treatment failure. In this work we focus on developing mathematical models to understand cancer evolution leading to metastasis and chemo-resistance with a special focus on the role of ITH. Our central goal is to understand the evolution of phenotypic heterogeneity as tumor cells

adaptation to various environments. We use a multiscale model to systematically study cancer metastasis and make connections to potential clinical implications for optimizing screening and treatment schedules. At the cell level, we use a cell-based model (the Cellular Potts Model or CPM) to simulate the collective cancer invasion. At the population level, we use continuous replicator dynamics to analysis the adaptation strategies of the tumor. This work reveals how the pairwise interactions between phenotypes within the tumor, together with the microenvironments, alter the dynamics of the tumor progression and change their responses to chemotherapy. The study will offer potential clinical prognosis information and treatment strategies for patients.

INDEX WORDS: Intratumor Heterogeneity, Collective Invasion, Cancer Metastasis, Drug Resistance, Evolutionary Game Theory, Allee Effect, Cancer therapeutic strategy

Modeling Evolution of Intratumor Phenotypic Heterogeneity in Metastasis and Cancer Drug Resistance

by

Bin Zhang

A Dissertation Submitted in Partial Fulfillment of the Requirements for the Degree of

Doctor of Philosophy

in the College of Arts and Sciences

Georgia State University

2021

Modeling Evolution of Intratumor Phenotypic Heterogeneity in Metastasis and Cancer Drug Resistance

by

Bin Zhang

Committee Chair: Yi Jiang

Committee: Jun Kong

Alexandra Smirnova

Adam Marcus

Electronic Version Approved:

Office of Graduate Services

College of Arts and Sciences

Georgia State University

May 2021

ACKNOWLEDGEMENTS

Firstly, I would like to express my sincere gratitude to my advisor Prof. Yi Jiang for the continuous support of my PhD study and related research, for her patience, motivation, and immense knowledge. Her guidance helped me in all the time of research and writing of this dissertation. I could not have imagined having a better advisor and mentor for my PhD study.

Besides my advisor, I would like to thank the rest of my thesis committee: Prof. Jun Kong, Prof. Adam Marcus, and Prof. Alexandra Smirnova, for their insightful comments and encouragement, but also for the hard question which incented me to widen my research from various perspectives. My sincere thanks also go to Prof. James Mac Hyman, Dr. Hao Chen, Dr. Sergey Klimov, Mr. Anthony Morciglio, and Dr. Karina Mazzitello, who provided me an opportunity to join their team and share their ideas, thoughts and who gave access to the laboratory and research facilities. Without they precious support it would not be possible to conduct this research.

Last but not the least, I would like to thank my family: my parents for supporting me spiritually throughout writing this dissertation and my friends who keep me accompany and help me a lot in general.

TABLE OF CONTENTS

ACKNOWLEDGEMENTS IV

LIST OF TABLES IX

LIST OF FIGURES X

1 INTRODUCTION 1

1.1 Hallmarks of Cancer 1

1.2 Cancer as an Evolutionary and Ecological Process 2

1.3 Project Description 3

1.3.1 Background *3*

1.3.2 Aims of Our Study *4*

1.4 Chapter Summaries 8

2 CELL-BASED MULTISCALE MODEL FOR COLLECTIVE INVASION WITH LEADER AND FOLLOWER CELLS IN NON-SMALL CELL LUNG CANCER.. 11

2.1 Abstract 11

2.2 Introduction 12

2.3 Models and Methods 14

2.3.1 Agent Based Model: Cellular Potts Model (CPM) *14*

2.4 Results and Conclusions 16

2.4.1 CPM suggests the existence of two distinct phenotypes is indispensable in collective invasion process. *16*

2.5 Discussion 20

2.5.1 Leader and Follower Cell Composition is Critical in Collective Invasion 20

2.6 Future Work 22

2.6.1 Leader-Follower Behaviors with Intermediate Phenotype 22

2.6.2 Leader-Follower Behaviors with Complex Ecological Factors 25

3 THE ECOLOGY OF COLLECTIVE CANCER INVASION INFORMS THERAPY STRATEGIES: AN EVOLUTIONARY GAME THEORY MODEL 27

3.1 Abstract 27

3.2 Introduction 28

3.3 Methods 29

3.3.1 Evolutionary game theory model for collective invasion 29

3.4 Results 33

3.4.1 Tumor growth and Leader-Follower Composition 33

3.4.2 Targeting Leader-Follower Interaction as A Novel Chemotherapy Strategy 37

3.4.3 Benefits of Drug Combination in Chemotherapy 40

3.5 Discussion 42

3.6 Conclusion 43

3.7 Supporting Information 45

3.7.1 Sensitivity of Pairwise Interactions to Collective Invasion Dynamics. 45

3.7.2 Stability Analysis 49

4 HOW ALLEE EFFECT IMPROVES THE PROBABILITY OF TUMOR ERADICATION IN RESPONSE TO CHEMOTHERAPY 52

4.1 Abstract 52

4.2 Introduction 53

4.3 Model 55

4.3.1 Tumor Growth Dynamics 56

4.3.2 Drug Resistance Evolution 57

4.3.3 Drug Efficacy 57

4.4 Results 58

4.4.1 Growth Rate per Capita 58

4.4.2 Treatment Protocol 59

4.4.3 Effect of Allee Threshold Versus Effective Drug Concentration 61

4.4.4 Disease Burden Versus Drug Concentration 63

4.4.5 Drug Resistance Versus Drug Concentration 63

4.5 Discussion 65

4.5.1 Benefits of Combination Chemotherapy 66

4.5.2 Benefits of Adjuvant Chemotherapy 67

4.5.3 Drug Strategies in Adjuvant or Progression-free Survival (PFS) Phase 67

5 MATHEMATICAL FRAMEWORK OF COMBINATIONAL CHEMOTHERAPY EFFECTS AND THE EVOLUTION OF RESISTANCE 69

5.1 Abstract 69

5.2 Introduction 70

5.3 Methods 71

5.3.1 The Effect of Combination Therapy 73

5.3.2 Spontaneous and Drug-induced Resistance 74

5.4 Results 75

6 CONCLUSIONS AND FUTURE WORK 78

6.1 Summary 78

6.2 Future Work 81

REFERENCES 85

LIST OF TABLES

Table 3-1 Parameters Used for the Evolutionary Game Model 31

Table 3-2 Three Protocols (Potential Targets) for Chemotherapy 40

Table 4-1 Parameters Used for the Model with Allee Effect 56

Table 5-1 Parameters for the Model Comparing Combination Chemotherapy Effects .. 73

LIST OF FIGURES

Figure 2-1 Experimental Observations of Leader-Follower Cells Behaviors in Collective Cancer Invasion[23] 13

Figure 2-2 Schematic Diagram of Cellular Potts Model and CompuCell3D[54] 16

Figure 2-3 CompuCell3D Simulation of Leader-Follower Cells Behaviors in Collective Cancer Invasion I 18

Figure 2-4 CompuCell3D Simulation of Leader-Follower Cells Behaviors in Collective Cancer Invasion II 19

Figure 2-5 CompuCell3D Simulation of the Tumor with All Follower and No Leader Cell 21

Figure 2-6 CompuCell3D Simulation of the Tumor with All Leader and No Follower Cells 22

Figure 2-7 Schematic Diagram of Notch-Delta-Jagged Signaling Pathway 24

Figure 3-1 Leader and follower ecosystem in collective invasion 29

Figure 3-2 Schematic Diagram of Evolutionary Game Theory Model with Various Pairwise Interaction Intensities 32

Figure 3-3 Tumor Dynamic of the Evolutionary Game Model I 34

Figure 3-4 Dependence of the tumor burden as measured by the tumor cell number ... 36

Figure 3-5 Coupled pairwise parameters influence the leader composition in the tumor I 37

Figure 3-6 Treatment Cost and its Efficacy of the Evolutionary Game Model I 39

Figure 3-7 Evolutionary Dynamics of the Tumor under Different Treatment Protocols .. 41

Figure 3-8 Evolutionary Dynamics of the Tumor under Different Treatment Protocols II 42

Figure 3-9 Influences of coupled parameters of the Evolutionary Game Model II 46

Figure 3-10 Influences of coupled parameters of the Evolutionary Game Model III 47

Figure 3-11 Influences of coupled parameters of the Evolutionary Game Model IV..... 48

Figure 3-12 Phase Diagram of the Evolutionary Game Model 51

Figure 4-1 Tumor Growth Dynamics with/without Considering Strong Allee Effect 59

Figure 4-2 Schematic of tumor dynamics under two treatment regimes..... 60

Figure 4-3 Schematic Diagram of the Treatment Strategy Selection and Tumor Growth Dynamics 61

Figure 4-4 Tumor dynamics under multiple effective drug concentrations and Allee thresholds 62

Figure 4-5 Tumor dynamics under multiple effective drug concentrations and initial tumor size 64

Figure 4-6 Tumor dynamics under multiple different growth models with constant dosage treatment 65

Figure 5-1 Schematic Diagram of Drug Interactions and Evolution of Multi-type Resistance during Chemotherapy 71

Figure 5-2 A Demo Drug Interaction (Synergy/Additive/Antagonism) Matrix 74

Figure 5-3 Evolution of Drug Resistance under Different Drug Interactions 76

Figure 5-4 Emergence of Resistance and Progression Survival under Different Drug Interactions 77

1 INTRODUCTION

1.1 Hallmarks of Cancer

Cancer, the second leading cause of death globally behind cardiovascular diseases[1], is an evolutionary disease. The understand of this disease is also evolutionary. Cancer is a dynamic complex multi-scale system that can only truly be understood via the integration of theory and experiments. Therefore, more and more researchers use such an integrated approach to better understand cancer initiation, progression, and treatment and to aid in the clinical utilization of integrated models in precision medicine. By using a range of mathematical modeling approaches targeted at specific types of cancer, it is beneficial in the development and testing of new treatment strategies as well as facilitating a deeper understanding of why they fail. This multi-model, multi-scale approach has led to a diverse and rich interdisciplinary to understand the disease and to create many insights resulting in novel approaches for the cancer treatment.

The seminal review papers by Hanahan and Weinberg proposed six hallmarks of cancer[2,3]: self-sufficiency in growth signals, evading apoptosis, insensitive to anti-growth signals, sustained angiogenesis, limitless replicative potential and tissue invasion & metastasis[3]; which they modified after one decade: sustaining proliferative signaling, evading growth suppressors, activating invasion and metastasis, enabling replicative immortality, inducing angiogenesis and resisting cell death[2]. Recognizing these concepts and their applicability will affect the development of new ways to treat cancer. This dissertation studies two of these hallmarks, invasion, and metastasis, and resisting cell death.

1.2 Cancer as an Evolutionary and Ecological Process

Ecology is a branch of biological science studying the dynamics of competition, cooperation, and interactions within a population with different level of fitness. There're multiple interactions types in ecological system, including competition, predation, mutualism, parasitism and etc[4–6]. This concept are extensively studied in describing a variety of biological interactions[7–9]. Tumor progression could be characterized as cooperators (i.e. healthy cells) take over the defectors (i.e. malignant cancer cells)[10,11] using evolutionary game theory models. Studying cancer as a clonal evolutionary disease could capture the dynamics of the tumor progression. There're multiple hypothesis describing the tumor evolution: linear, branching, neutral and punctuated[12]. This evolution is critical to reshape the intratumor heterogeneity, therefore has influences on treatment responses, metastatic potentials and results in different risk stratifications clinically[13]. This evolution could result in different phenotypes in chemosensitivity[14] and metastasis[15]. While therapy can alter the competition[16,17] and selection pressure between healthy cells, sensitive cells and resistant cells with different fitness. Mathematical modeling has successfully and are desired[18] to better understand the evolutionary nature of therapeutic resistance, relapse of cancer as well as metastasis[19]. This dissertation is focused on building a multi-scale mathematical framework to model the evolution dynamics of the cancer in respect to chemosensitivity and metastatic processes.

1.3 Project Description

1.3.1 Background

Cancer is the second leading cause of death globally behind cardiovascular diseases[1]; its development mirrors and evolutionary process in species[2,5]. This disease exhibits tremendous genomic and phenotypic heterogeneity. The intratumor heterogeneity is one of the major barriers for successful treatments, leading to different chemotherapy sensitivity[16,17,20–22] and increase the metastatic potential[23], two main causes of cancer death[24,25]. The genomic heterogeneity has been extensively studied with the advent of the state-of-art sequencing techniques and yield amounts of clinical applications, including targeted chemotherapy agents, prognosis biomarkers and etc. On the other hand, the study of phenotypic ITH has offered the opportunity to understand how tumor adapts to different environments, selection pressure, or therapeutic treatments. This understanding will help to design optimal treatment regimen strategies and schedules to combat cancer and manage its progression.

Metastasis is one of the hallmarks of the cancer[2], when some tumor cells break off from the original tumor, seed in other tissues or organs and form secondary tumors. Drug resistance, either intrinsic (pre-existing) or drug-induced, is responsible for ineffective treatment of the cancer, resulting in relapses and eventual patient death. Study of these two processes proceed along as separate pathways in the previous research[20,25–28]. However, current researches reveal some correlations between drug resistance and cancer invasion[29,30]. To overcome these two major impediments of cancer treatment, metastasis and drug resistance, we need to understand the evolution

dynamics of ITH. Therefore, it's natural to stratify the tumor cells into subpopulations, sensitive and resistant or localized and migratory subclones.

Advances in experimental techniques of distinguishing various phenotypes in collective cancer invasion[23] are calling for innovations of mathematical modeling. A recent study using an image-guided genomics approach (SaGA) identified the existence of at least two distinct phenotypes in non-small cell lung cancer (NSCLC) invasion packs: highly migratory leader cells (L) and highly proliferative follower cells (F)[23,31]. Experimental data reveal that the leader cells provide escape mechanisms for the followers, and follower cells in turn provide leader leaders with increased growth and survival. These phenotypically distinct cell types cooperate to promote cancer invasion[23,31].

1.3.2 Aims of Our Study

We will integrate experimental and modeling investigation of cancer phenotypes dynamics and evolution in disease progression with the following aims:

Aim I: Study Cellular Mechanisms Leader-Follower Interactions and Simulate Leader-Follower Behaviors in Collective Invasion with CPM

In collaboration with Dr. Adam Marcus' lab from Emory Winship Cancer Institute, we observed the existence of at least two phenotypes: leader and follower cells in non-small cell lung cancer. Leader cells, highly migratory and less proliferative, and follower cells, highly proliferative but less migratory, constitutes the collective invasion packs of a tumor spheroids in vitro. These phenotypes differ not only in collective invasion behaviors but also in genetical aspects, where the differential expression analysis

further confirms this discrepancy in consistence with the bifurcation analysis of the N-D-J dynamics, where leaders cells have high expression of JAG1[23].

Thus, we propose to develop a multiscale collective invasion model which takes into consideration of two phenotypes, leader and follower cells. Cellular Potts Model (CPM)[32,33] will be applied to explain the observed collective invasion phenomena in H1299 spheroid in vitro[23]. We explore the minimum conditions to form the model and explain the essence of the existence of leader and follower cells in collective invasion. Furthermore, this model setup will serve as a testbed and framework to study the collective invasion by incorporating the detailed cellular interactions[23,34], extracellular matrix interactions[31,35] and other physical and biological factors. Meanwhile, the collective invasion efficacy can be assessed by quantifications of invasion packs, invasion radius and etc[36].

Aim II: Understand the Roles of Phenotypes (Leader and Follower Cells) and Their Pairwise Interactions (Cooperation and Defection) in Collective Invasion Dynamics

With the establishment of the cell level model, we show the essence of the existence of the different phenotypes in collective invasion regarding of the invasion time scale (around 24 hours in vitro for NSCLC H1299 cell line). We need to explore the phenotypic ITH evolution in collective invasion process and understand the pairwise interactions between leader and follower cells. We propose an evolutionary game theory (EGT) framework to study the role of leader and follower cells. Therefore, it's simple to characterize the pairwise interactions by a payoff matrix and build a replicator dynamics system to analysis the evolution of phenotypic ITH.

The replicator system reveals the fraction of leader cells, which is a possible clinical implication to characterize the potential of metastasis, and the total number of tumors. By conducting sensitivity analysis, we model could point out the most effective strategies in lowering disease burden as well as metastasis potential. Linking these strategies with the pairwise interactions could identify the novel targets to design chemo-agents and may make possible clinical implications for overcoming the barriers of the successful treatments.

Aim III: Establish a Framework to Model Tumor Progression with Spontaneous and Drug-induced Resistance and Understand how Treatments Influence the Emergence of Resistance

Another barrier for successful cancer treatment is chemoresistance. We propose a continuous cell-population model to analysis the evolution of drug resistant phenotype. The existence of pre-existing and the acquisition of chemo-resistance during treatment are critical in patient outcomes[20,21,37].

First, we need to quantitatively understand the role of pre-existing resistance and how this reshapes the cure of the cancer. Tumor growth dynamics are described as exponential, logistic growth, Gomperzian models[38] and etc. using ordinary differential equations (ODEs). One of the limitations of these model is that they're not capable to capture the dynamics at a low cell density[39]. We incorporate Allee effect into the model and extend the understanding explore the dynamics of the tumor progression in low disease burden. We propose to use this framework to analysis the cure rate related to the proportion of the pre-existing resistance. Also, this piece of work will shine light upon

the management, treatment and screening strategies in clinical practices when the patient has a very low tumor burden or even is in disease-free status.

Then, we apply this framework to study the interactions of drug, synergy, antagonism, additive. The discrepancies of the drug interactions in treatment schedule could shape the evolution phenotypical ITH, such as the emergence time for the resistant subclones, the composition of the tumor, the overall fitness of the tumor and etc. By combine these aspects included in the model, we can explore the potential optimal treatment schedule and strategies for a low side effects, long progression survival and delaying emergences for chemo-resistance scenario.

This work will analysis the dynamics of the phenotypical ITH in the process of collective invasion and treatments under different regimens of chemotherapy. The study motivation is to understand the evolution of phenotypical ITH, a characterization indicates the tumor's adaptation to different environments or selection pressures. This work will reveal how the pairwise interactions between phenotypes within the tumor, together with the microenvironments, alter the dynamics of tumor progression and potential clinical prognosis of the patients. Furthermore, with the combination of chemosensitivity phenotypic evolution, the model will offer a testbed for the optimal treatment schedule design and develop new strategies or implications in clinical practices.

1.4 Chapter Summaries

In chapter 2 of this dissertation, the behaviors and phenomena of collective cancer invasion in vitro are studied. The experiments distinguished leader cells and follower cells in both behaviors and genomic differences[23,27,31] and confirms the existence of at least two distinct phenotypes. Then we introduce a Cellular Potts Model (CPM) to establish a framework to depict the phenomena emerged in collective cancer invasion spheroids for non-small cell lung cancer cell line in vitro. This framework can serve as a testbed to incorporate the biological details, such as pairwise interactions between leader cells and follower cells[31], interaction with extracellular matrix[35,40–42] and etc.

In chapter 3, an evolutionary game theory model is applied to the collective cancer invasion system to study how the pairwise interactions within the collective spheroid reshape the intratumor heterogeneity. A payoff matrix and a replicator dynamic system is established to characterize the fraction of highly migratory and highly proliferative subpopulations, which have possible clinical links to metastatic potential and tumor burden. Furthermore, by targeting different pairwise interactions, the effects of the treatments are different. This model reveals novel target may be beneficial in reducing metastatic potential as well as tumor burden and shine light upon optimal chemotherapy regimens.

In chapter 4, another impediment of successful cure of cancer is discussed. The dynamics of tumor growth are extensively studied for decades[43–46]. However, recent experiments which examine the tumor cell population at low cell density reveal the

growth dynamic deviate from exponential growth pattern and indicate an Allee effect in vitro[39]. This effect is expected to be much stronger in vivo[39] and could result in significant understanding of tumor progression. We adopt Allee effect and analyze the tumor growth dynamics and response under treatments. This model could explain the cure of cancer by chemotherapy and characterize the leading factors yielding successful chemotherapy treatments. Furthermore, this offers a strategy and insight in managing, screening and choosing proper treatment for either complete cure or prolong patients' survival and life qualities depending on situations at diagnosis.

In chapter 5, the usage of combinational chemotherapy and drug interactions are discussed. The seeking for optimal chemotherapy regimens is critical in clinical practices, the optimal choices of a combinational chemotherapy agents and proper administration could result in different outcome for the patients. We propose a simple set of ordinary differential equations to quantify the effects of drug interactions: synergy, additive, and antagonism. The drug interactions lead to different evolutionary trajectories of phenotypic intratumor heterogeneity (ITH), thus resulting in different treatment outcomes. This framework suggests the synergy effect, in short term, could efficiently reduce the tumor cell number (disease burden), but the trade-off, compared with antagonism drug combinations, is the earlier emergence of drug resistant subclones. This conclusion is essential and critical in formulating combinational chemotherapy schedules and managing tumor progression of the patients.

In chapter 6, an outline of the future work beyond the scope of dissertation is listed which could be explored to have a more comprehensive understanding of the

evolution of phenotypic ITH during cancer progression, more relevant to clinical practices and may become exciting directions for future research.

2 Cell-based Multiscale Model for Collective Invasion with Leader and Follower Cells in Non-small Cell Lung Cancer

2.1 Abstract

Cancer is an evolutionary disease which exhibits genomic and phenotypic heterogeneity. Collective cancer invasion, where cells invade into peritumoral stroma as a cohesive and polarized mass maintaining cell-cell contacts, is shown to associate with better metastatic success and poor patient outcome. Recent experiments revealed two distinct phenotypes, leaders and followers, in non-small cell lung cancer during collective invasion. Even though we have identified distinct phenotypes in the collective invasion pack, the interactions between the phenotypes and between cells and the microenvironment have not been well understood. We adopt a cell-based multiscale model to depict the phenomena emerged in collective cancer invasion spheroids for non-small cell lung cancer cell line in vitro and explore the minimal conditions to form collective invasion packs. We confirm the existence of two distinct phenotypes is indispensable in collective invasion process by Cellular Potts Model. This framework can serve as a testbed to incorporate the biological details, such as pairwise interactions between leader cells and follower cells, interaction with extracellular matrix etc.

2.2 Introduction

Non-small cell lung cancer (NSCLC) constitutes 80% to 85% of lung cancers causing 120,000 deaths per year in the United States[47]. One major impediment of successful treatment is the intratumor heterogeneity at the genomic and epigenomic levels which leads to differential chemotherapy sensitivity and metastatic potential[16,17,20,21]. These subclones together with the microenvironment form a complex multi-cellular ecosystem[31]. The evolution of the tumor and environmental selection alter the tumor dynamics and have important consequences on tumor growth and its response to the treatments.

Using an image-guided genomics approach termed SaGA, we can precisely select live cells in space and over time, and subject them to genomic analysis[23]. Collective invasion occurs spontaneously from spheroids embedded in collagen. Each collective invasion pack consists of at least two distinct cell types, the leader at the tip of pack followed by follower cells. In most cases, when leaders detach, the packs cease to invade (Fig 1B), indicating the important role of leader cells in driving collective invasion. Using SaGA on collectively invading cancer cell packs, we created novel purified leader and follower cell lines from heterogeneous cell population. The leaders are more motile and less proliferative; they are also phenotypically stable, stay as leaders for >2 years. The followers are proliferative and minimally invasive. Leaders emerge from followers in about 2 months. Genomic and molecular analyses show leaders enrich VEGF, focal adhesion and Notch signaling. Leaders also overexpress VEGFR1 and VE-cadherin, DII4 and Jag1, suggesting that leaders and followers cooperate via VEGF-activated Notch/Delta/Jagged and Cadherin signaling pathways[23].

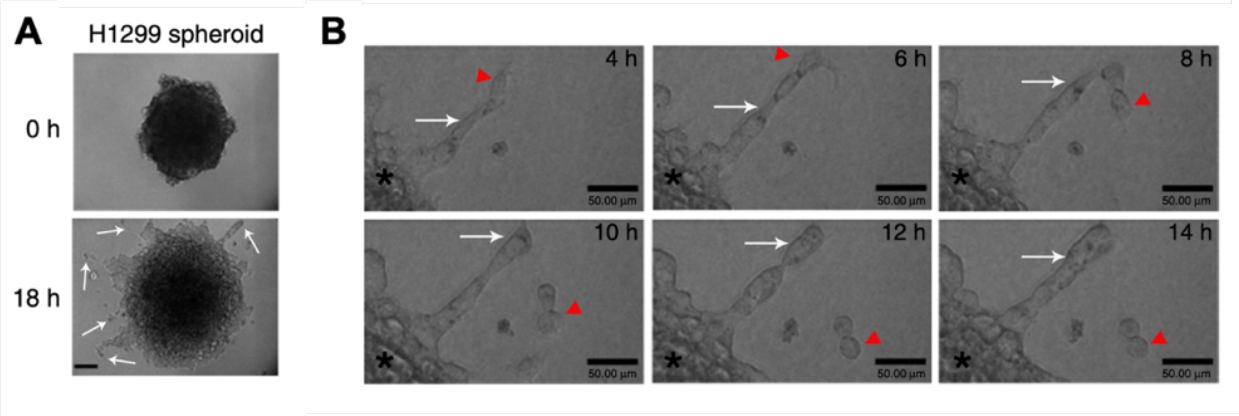

Figure 2-1 Experimental Observations of Leader-Follower Cells Behaviors in Collective Cancer Invasion[23]

(A) H1299 spheroid embedded in collagen was imaged at 0h (top) and 18h (bottom) post embedding. Arrows, leader-follower invasive chains[23]. (B) Time lapse of H1299 spheroids imaged using live cell confocal imaging every 2h. Arrow, follower cells in invasive chains; red arrowhead, leader cells[23].(Reproduced with permission from Konen, J et al. Nat. Commun. 8, 1-15 2017)

The usage of mathematical models to explain and make predictions to biological processes is one of a major branches of life sciences research nowadays. Cancer is a dynamic complex multi-scale system[17,18,38] and an evolutionary disease[7,18,48,49] that can be truly understand via the integration of theory and experiments. Therefore, more and more researchers implement this integrated methods to explore and gain comprehensive understanding towards cancer initiation[7,10,46], progression and treatments[20,50,51] and to aid in the clinical utilization in personalized medicine[25,38,52]. By using a range of mathematical modeling tools, it is beneficial in developing and testing novel treatment strategies as well as acquiring the deeper insights of why the treatments success or fail.

In this study, we adopt an agent-based model to explore the leader-follower behaviors in collective invasion of NSCLC. We explore a preliminary cell-based multiscale model with minimum conditions to reproduce the experiment phenomena in vitro.

2.3 Models and Methods

2.3.1 Agent Based Model: Cellular Potts Model (CPM)

Cellular Potts model (CPM)[33,53,54] is an cellular-level agent based model developed to simulate tissue growth and movement.

The implement of CPM is by projecting cell on a lattice. Each lattice site is named as pixel has an index number (shown in Fig 1.2A). All sites with the lattice index σ represent a separate cell. Therefore, such pixels could have contact with other pixels belonging to a different cell, this connection induces an energy penalty. In a typical CPM Model, cells have defined volumes, areas and interact with adhesion, thus this energy penalty can be written as[53]

$$H_{Contact} = \sum_{i,j\ neighbors} J(\tau_{\sigma_i}, \tau_{\sigma_j})(1 - \delta(\tau_{\sigma_i}, \tau_{\sigma_j})) + \sum_{\sigma} [\lambda_{Vol}(\sigma)(v(\sigma) - V_{target}(\sigma))^2]$$

The first term of the energy is due to contact, where J is the relative strength of the adhesion between different cells. The second term in the energy penalty is a constraint for cell volume (3D) regulation (while in 2D, it's defined as targeted surface areas). This term enables the model to simulate cell growth over time.

Chemotaxis can be added to this model with additional fields to describe the concentration $C(x, y, z)$ of the signaling agents, therefore it enables the movement of the cells in CPM. The energy associate with chemotaxis is determined by

$$H_{Chemical} = \mu(\sigma)C(x, y, z)$$

where $\mu(\sigma)$ is the effective chemical potential and $C(x, y, z)$ is the concentration of the chemicals. This term leads to the cell's biased motion along the concentration gradient of the chemotaxis agent.

Another important parameter in this CPM is temperature, which determines the fluctuation strength of cell membranes. Figure 1.1A illustrates the process of the membrane fluctuation: each Monte Carlo step, a pixel is selected, if this proposed change in the configuration induces a variation in energy ΔH, the probability of the system accepts this change is given by

$$H = H_{Contact} + H_{Chemical}$$

$$P(\Delta H) = min(1, e^{-\Delta H/kT})$$

where kT is the thermo energy; the higher the temperature, the higher probability of accepting membrane fluctuations.

Additional properties of the cell behaviors can be added to this model, which modifies the energy penalty. James Glazier's group developed a software named CompuCell3D implementing CPM and combined various features describing cellular properties for multi-scale biological system modeling. With the wide applications of CompuCell3D, cell sorting[33], tissue-level mechanics[35,55–57] (extracellular matrix (ECM) interactions), tumor growth[58,59], invasion[60] and evolution[32,61] and a variety of biological systems[62,63] can be modeled under this framework. We adopted this framework to establish a preliminary multi-scale model to describe the leader follower cells collective invasion phenomena in non-small cell lung cancer (NSCLC) cell line H1299[23].

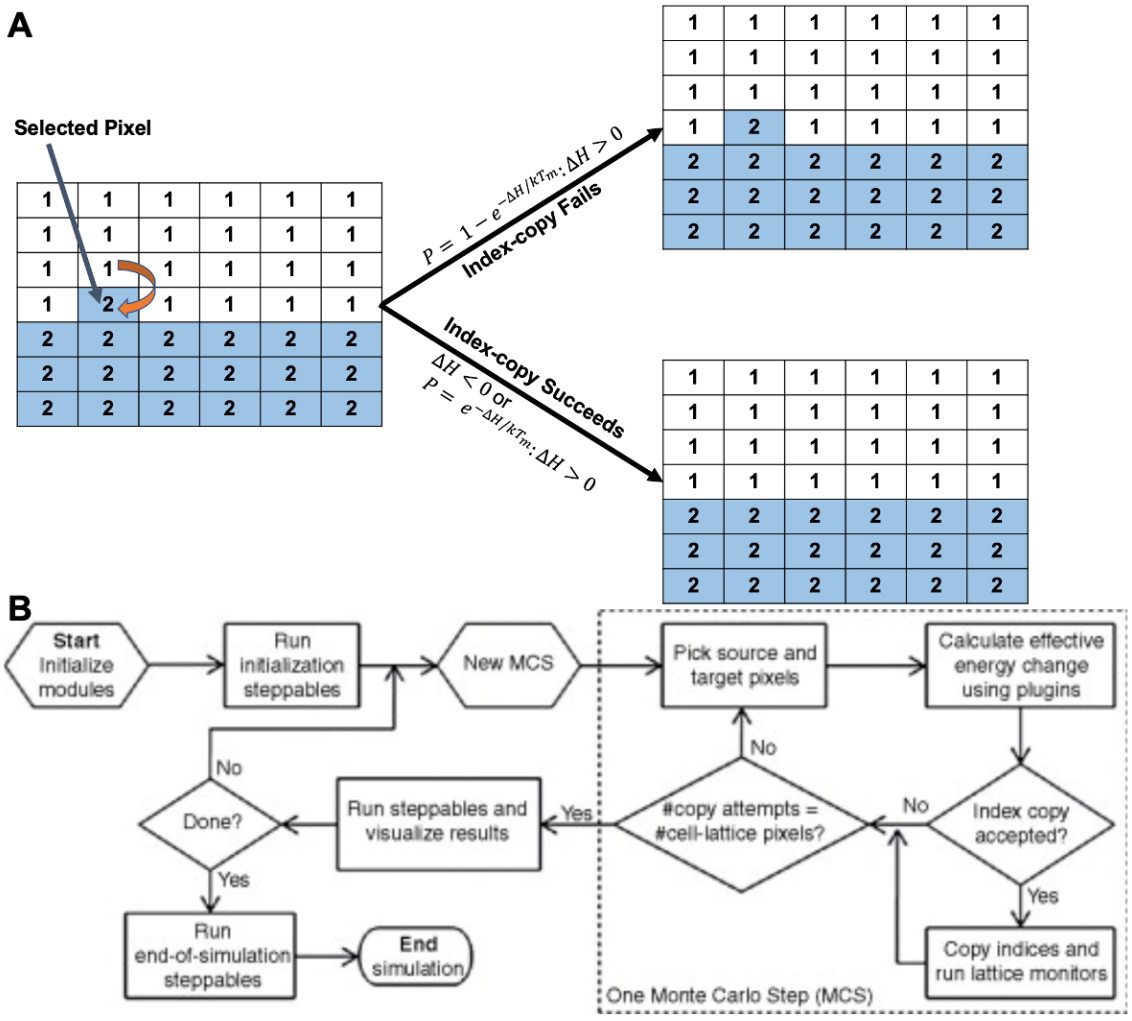

Figure 2-2 Schematic Diagram of Cellular Potts Model and CompuCell3D[53]
(A) Illustration of Cellular Potts Model (CPM) on a lattice, 1 stands for cell with id one and 2 for cell with id 2, and the index-copy process is by evaluating the Hamiltonian. (B) Flowchart of the CompuCell3D, an implementation software of Cellular Potts Model. *(Reproduced with permission from Swat, M. H. et al. Modeling of Tissues Using CompuCell3DMethods. 325-366 2012)*

2.4 Results and Conclusions

2.4.1 CPM suggests the existence of two distinct phenotypes is indispensable in collective invasion process.

To understand the roles and contributions of the leader cells and follower in the collective invasion process, we are exploring the minimum requirements or assumptions

for establish a preliminary cell-based multiscale model. We adopt CPM and CompuCell3D as our theoretical framework to capture the phenomena in collective cancer invasion process.

The time scale for the modeling is the typical time, 24 hours (1 day), for the experiments' observations for collective invasion, therefore, the tumor cell proliferation effects can be ignored during this period of simulation time scale. We set up minimum conditions for establishing CPM; contact adhesion and chemotaxis to simulate collective invasion process. The contact adhesion is applied to capture the membrane fluctuation, which provides the general rule for the cellular level membrane fluctuation. The adhesion coefficient is set differently for leader cells and follower cells, where the leader cells have stronger adhesion to follower cells than to other leader cells. The chemotaxis is set to provide the migration source for the leader cells; only leader cells react to the chemotaxis agent while the follower cells don't. The time step in the simulation setup is Monte Carlo Steps (MCS), we match the MCS with the time in experiment based on the migration distance of the leader cells: in 10 hours the directional migration length is 50 microns[23], therefore in the simulation, the average MCS for the leaders to directional migrate to 50 microns (approximately equivalent to 50 pixels length in the simulation) is matched as 10 hours.

Since the system we're modeling is radically symmetric, therefore we can simulate a two-dimensional space with only a quartan. If we only consider these two basic properties of the simulation and assign a relative low proportion of leader cells (depicted as green cells). The simulation can capture the phenomena observed in experiments[23,27]:

1. Leader cells emerge at the surface of the tumor.

2. Leader cell can lead a collective pack with follower cells behind it and forming a finger shape collective invasion pack.
3. Each invasion pack is led by only one leader cells, and when several leaders compete for an invasion pack tip position, only one leader retain at the tip, while the other leader cells detached from the collective invasion pack.
4. When the leader cells detached from the tip of the collective invasion pack, the collective invasion of this pack is shunted.

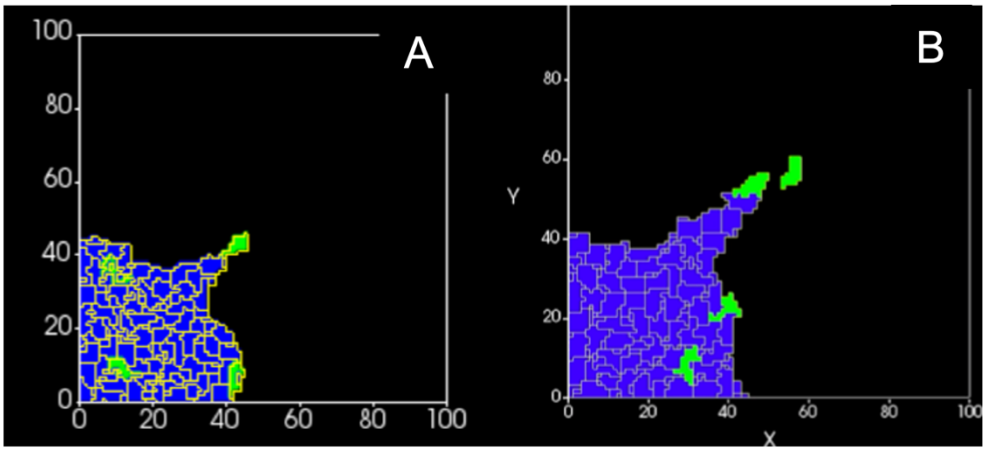

Figure 2-3 CompuCell3D Simulation of Leader-Follower Cells Behaviors in Collective Cancer Invasion I
Time lapse of cluster of cancer cells with leader (green) and follower (blue) cells with CC3D simulation.

When we alter the proportion of the leader cells to extreme cases, say $x_L = 1$ or $x_L = 0$, our simulations reveal the failure of collective invasion in a short time scale:

1. When all the cells are follower cells, the cells tend to harbor at their original positions and acts as Brownian motion (the membrane fluctuation intensity depends on the temperature of the simulation);

2. While on the other extreme situations, when all the cells are leader cells, the tumor will be unstable and separated as single cells with high migration ability, which is not the collective invasion behaviors.

Therefore, we can conclude the existence of the two distinct phenotypes, leader cells and follower cells, are critical and essential to form collective invasion in NSCLC by our simulation results. Advanced experiment techniques allow the selection of leader or follower cells, and experiments confirms the results generated by experiments, all leader cells or all follower cells cannot form collective invasion in this several tens of hours' time scale.

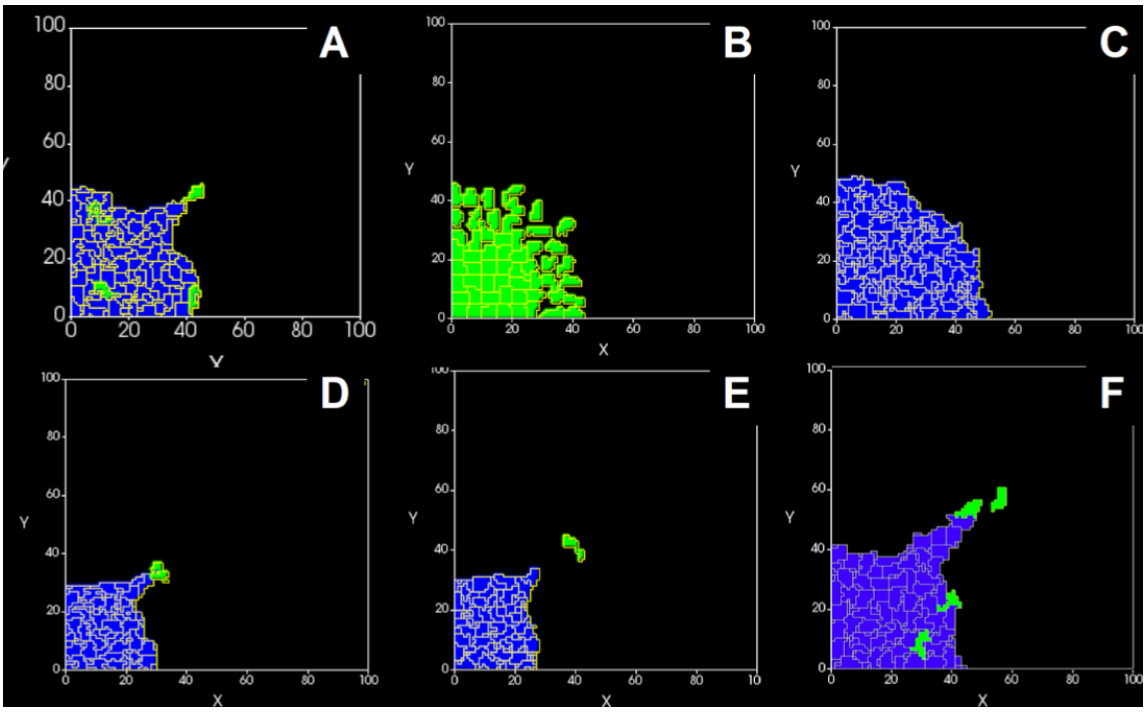

Figure 2-4 CompuCell3D Simulation of Leader-Follower Cells Behaviors in Collective Cancer Invasion II

2.5 Discussion

2.5.1 Leader and Follower Cell Composition is Critical in Collective Invasion

Follower cells, which have low capability in migration but high in proliferation, are the majority contribute to tumor growth, while the leader cells are equipped with high ability for migration providing the escaping mechanism from the primary sites. The existence of these distinct phenotypes is indispensable in collective invasion.

Intuitively, we consider two extreme scenarios of the tumor: one with all the follower cells and the other one with all leader cells. In these simulations, we consider a time scale of 24 hours to several days (typical collective invasion time scale for the tumor spheroids in vitro) and no phenotypic conversion between leader cells and follower cells.

1. All follower cells tumor: Fig 2-5 shows the simulation of the tumor with pure follower cells. Those cells are located at the primary sites and no collective invasion pack is formed. This simulation further confirms the existence of at least two distinct phenotypes in migration is necessary to form collective invasion. Otherwise, all follower cells will result in a benign tumor.
2. All leader cells tumor: Fig 2-6 shows the simulation of the tumor with pure leader cells. Those cells cannot form a cluster and invade to other sites individually. Recent study indicate the tumor cells need cooperation to grow at low cell density[39,64,65] or forming a metastatic site[65–67].

Therefore, phenotypic intratumor heterogeneity is favored in cancer evolution and progression. Leader cells provide escape mechanism for followers, follower cells in turn provide leaders with increased growth and survival. These phenotypically distinct cell

types cooperate to promote the escape. Thus, the existence of the mechanism of the phenotypic conversion is a key factor of the tumor malignancy.

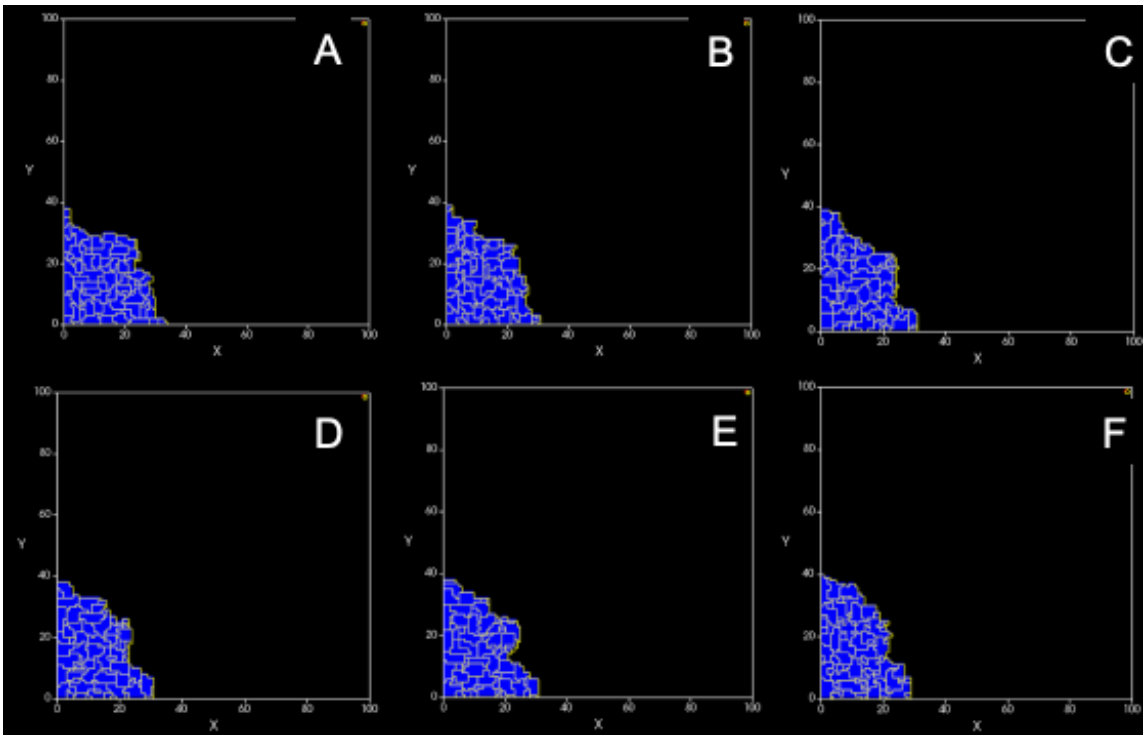

Figure 2-5 CompuCell3D Simulation of the Tumor with All Follower and No Leader Cell

Time lapse of the simulation of a cluster of cancer cells with only follower (blue) cells, the spheroid of the cancer maintains its shape and stay at its original position. This simulation reveals that the collective invasion cannot be formed by only follower cells.

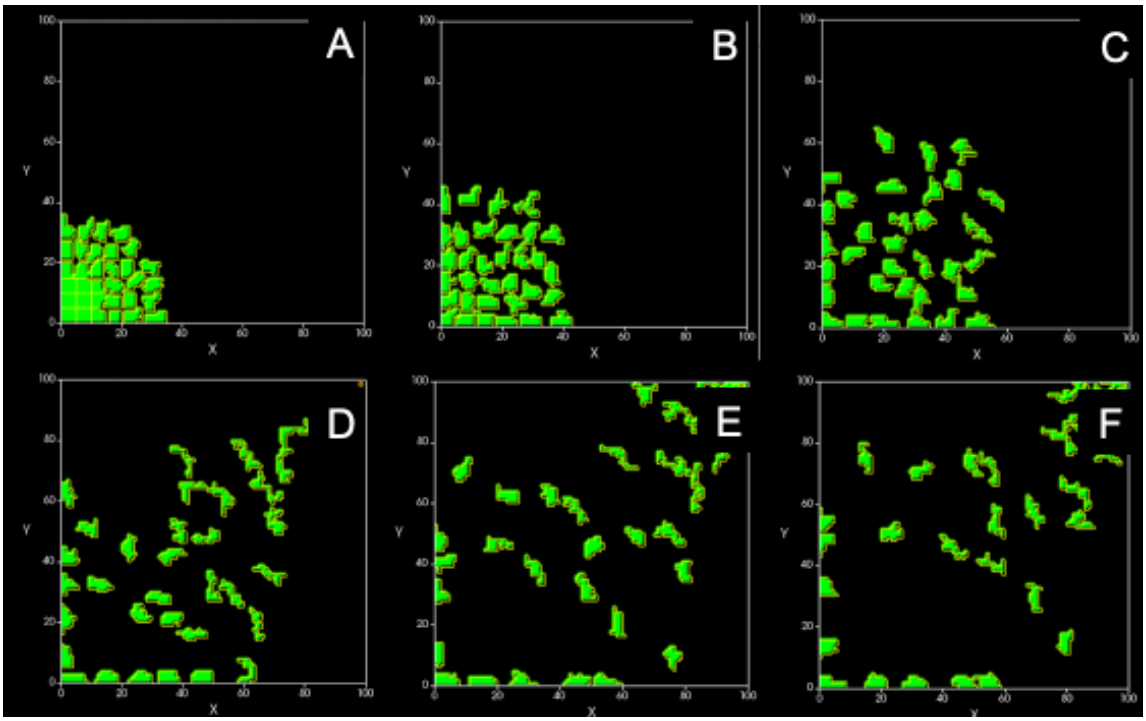

Figure 2-6 CompuCell3D Simulation of the Tumor with All Leader and No Follower Cells

Time lapse of the simulation of a cluster of cancer cells with only leader (green) cells, the spheroid of the cancer maintains breaks down and form individual invasion. This simulation reveals that the collective invasion cannot be formed by only leader cells.

2.6 Future Work

2.6.1 Leader-Follower Behaviors with Intermediate Phenotype

Collective invasion occurs when clusters of cells migrate into tumor stroma while maintaining cell to cell adhesion, mimicking sprouting angiogenesis in both morphology and VEGF/Notch/Delta signaling. Two phenotypes were observed in collective invasion: Leader and Follower. A recent paper proposes the emergence of a third, intermediate phenotype in angiogenesis. We ask if such an intermediate phenotype exist in the collective invasion of lung cancer (NSCLC).

Angiogenesis is the process of the new blood vessel formation from the existent ones. This process is critical in a huge amount of biological process, such as embryonic development, tumor metastasis[68] and homeostasis[34,69]. The signaling pathway of angiogenesis is extensively studied with Notch-signaling[34,70]. We adopt this framework and mimic sprouting angiogenesis. We establish compartments Notch (N), Delta (D), Jagged (J), Notch intracellular domain ($NICD: I$), Vascular endothelial growth factor (VEGF) receptors (V_R) and VEGF (V) to study the collective invasion process in NSCLC. The dynamics of the system is described as the following six ordinary differential equations (ODEs):

$$\frac{dN}{dt} = N_0 H^{S+}\left(I, \lambda_{I,N}\right) - N\left[(k_C D + k_T D_{ext}) H^{S+}\left(I, \lambda_{F,D}\right) + (k_C J + k_T J_{ext}) H^{S-}\left(I, \lambda_{F,J}\right)\right] - \gamma D$$

$$\frac{dD}{dt} = D_0 H^{S-}\left(I, \lambda_{I,D}\right) H^{S+}\left(I, \lambda_{V,D}\right) - D\left[k_C H^{S+}\left(I, \lambda_{F,D}\right) N + k_T N_{ext}\right] - \gamma D$$

$$\frac{dJ}{dt} = J_0 H^{S+}\left(I, \lambda_{I,J}\right) - J\left[\left(k_C H^{S-}\left(I, \lambda_{F,J}\right) N + k_T N_{ext}\right)\right] - \gamma J$$

$$\frac{dI}{dt} = k_T N\left[D_{ext} H^{S+}\left(I, \lambda_{F,D}\right) + J_{ext} H^{S-}\left(I, \lambda_{F,J}\right)\right] - \gamma_S I$$

$$\frac{dV_R}{dt} = V_{R_0} H^{S-}\left(I, \lambda_{I,V_R}\right) - k_T V_R V_{ext} - \gamma\, V_R$$

$$\frac{dV}{dt} = k_T V_R V_{ext} - \gamma_S V$$

[34]where γ represents the degradation rates of N, D, J, V_R, I, V, and the $N_0, D_0, J_0, V_R 0$ represent the innate production rates of the corresponding compartments. $N_{ext}, D_{ext}, J_{ext}, V_{ext}$ stand for the external compartments and k_C, k_T serve as the cis-inhibition and trans-inhibition rates of Notch with its ligands. The activation process of the system is characterized with shifted Hill functions H^S with a combination of inhibitory and

excitatory Hill components as $H^S(X, \lambda_{X,Y}) = H^-(X) + \lambda_{X,Y} H^+(X)$. The computation and bifurcation analysis is done by PyDSTool[71].

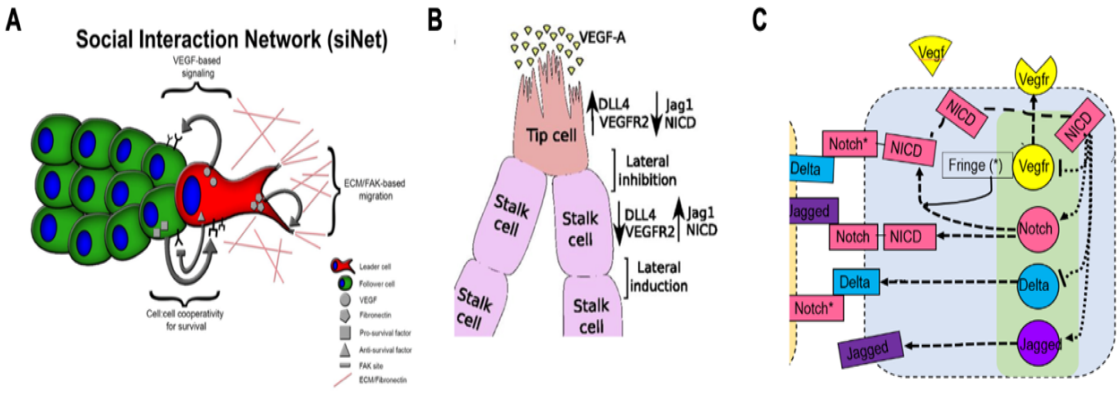

Figure 2-7 Schematic Diagram of Notch-Delta-Jagged Signaling Pathway

Signaling pathway dynamics analysis suggests the existence of at least two distinct phenotypes, we name it leader and follower cells, contributed to collective invasion process, which can be distinguished by Jagged expression. The cell can adopt phenotype at low levels of D_{ext} as leader cells, while follower cells at high levels of D_{ext} and intermediate D_{ext} and high expression of Jagged. Therefore, the angiogenesis model implicates at least two distinct phenotypes in collective invasion process. The genomic analysis further confirmed these two phenotypes: leader cells over-express JAG1 by RNAseq analysis than follower cells.

Anthony et al mimic this Notch-Delta-Jagged signaling network in angiogenesis process[34,69] and conduct a bifurcation analysis[71] and proposal the existence of multiple phenotypes evolved in collective invasion process. With a mathematical model of VEGF-activated Notch/Delta/Jagged signaling pathways, we determine the conditions for the intermediate phenotype. The results show that at overexpression of Jagged

(Jag1) and high secretion of VEGF from the leader, its neighboring cells can adopt the immediate phenotype.

This bifurcation analysis of Notch-Delta-Jagged signaling pathway suggests the existence of intermediate phenotypes between leader and follower cells in collective cancer invasion. The model can be extended to three phenotypes naturally, leader with high ability in migration but low in proliferation, follower with high proliferation but low in migration, and the intermediate phenotypes have the properties in between these two extreme tumor types. Under this cell-based multiscale model, we can explore the role of the existence of the intermediate phenotype and how it reshapes the collective invasion.

2.6.2 Leader-Follower Behaviors with Complex Ecological Factors

Leader and follower cells subclones together with the microenvironment form a complex multi-cellular ecosystem[31]. Additional properties can be added to the model, including pairwise interactions[23,27,31] between distinct phenotypes (leader and follower cell), interaction with extracellular matrix[35,40,54] and a variety of detailed biological factors.

Recent experiments using SaGA, a fluorescent imaging technique, observe leader and follower behaviors in NSCLC spheroids in vitro[23,27]. These two distinct phenotypes exchange signaling molecules[31] to coordinates leader-follower behaviors in collective invasion. The leader provides escaping mechanism for the followers and follower cells can secrete an undefined proliferation signal to promote the growth of leader cells, confirmed by experiment observation that the follower-only media increases leader cells proliferation rate[23]. Leader cells secrete VEGF, which is taken up by follower cells and

results in follower cells to follower them. However, the leader cells can secrete a growth inhibitor that reduces the proliferation rate of the follower cells. These complex pairwise interactions could enrich the dynamics of leader-follower behaviors in collective invasion, which can be incorporated to this agent-based model framework.

Other than these pairwise interactions mentioned above, fibronectin, one of the important biological molecules forming extracellular matrix[72], secretion by leader cells can expand the leader cells' domain, therefore relax the competition pression on leader cells proliferation[31]. Ordinary differential equations model predicts that when altering the signaling environment, the relationship of the cell types and the development of the complex system can be altered[31]. We can embed the extracellular matrix (mainly fibronectin) in the framework and explore the dynamics of the collective invasion with spatial information. This information is crucial and will enrich our understanding towards collective cancer invasion may shed light on potential applications in clinical settings, such as diagnosis, novel target chemo-agents preventing metastasis etc.

3 The Ecology of Collective Cancer Invasion Informs Therapy Strategies: An Evolutionary Game Theory Model

3.1 Abstract

Tumors, as they grow, consist of cells with increasing genomic and phenotypic heterogeneity. Together with the tumor microenvironments, the cell subclones within the tumor form a complex multi-cellular ecosystem. Specialized phenotypic subclones adapt to changing environmental conditions and influence the response to treatments. We found two distinct phenotypes in non-small cell lung cancer cell spheroids, leader and follower, that are responsible for collective invasion. Here, we use an evolutionary game theory framework to model the interactions between leader and follower cells and with the microenvironment. Measuring the total tumor burden and the leader fraction that drive collective invasion, we show that the pairwise interactions between leader and follower cells alter the collective dynamics: cooperation and defection can both promote collective invasion, while defection reduces tumor burden. These findings suggest potential new treatment strategies that target leader and follower cell-cell interactions. We show that combination treatment strategies could reduce tumor burden as well as lower the risk for collective invasion.

3.2 Introduction

Non-small cell lung cancer (NSCLC) constitutes 80% to 85% of lung cancers causing 120,000 deaths per year in the United States[47]. One of the main barriers for successful treatment is the tumor heterogeneity at the genomic and epigenomic levels which leads to differential chemotherapy sensitivity and metastatic potential[16,17,20,21]. These subclones together with the microenvironment form a complex multi-cellular ecosystem[31]. The evolution of the tumor and environmental selection alter the tumor dynamics and have important consequences on tumor growth and its response to the treatments.

Collective invasion occurs spontaneously from NSCLC spheroids embedded in collagen (Fig 1A). Approaches that homogenize large cell populations, in both clinical and pre-clinical models, cannot resolve the molecular signatures or phenotypes of rare or heterogeneous cell subtypes that can drive tumor progression. Using an image-guided genomics approach termed SaGA, we can precisely select live cells in space and over time, and subject them to genomic analysis[23]. Collective invasion occurs spontaneously from spheroids embedded in collagen (Fig 1A). Each collective invasion pack consists of at least two distinct cell types, the leader at the tip of pack followed by follower cells. In most cases, when leaders detach, the packs cease to invade (Fig 1B), indicating the important role of leader cells in driving collective invasion. Using SaGA on collectively invading cancer cell packs, we created novel purified leader and follower cell lines from heterogeneous cell population (Fig 1C). The leaders are more motile and less proliferative; they are also phenotypically stable, stay as leaders for >2 years. The

followers are proliferative and minimally invasive. Leaders emerge from followers in about 2 months. Genomic and molecular analyses show leaders enrich VEGF, focal adhesion and Notch signaling. Leaders also overexpress VEGFR1 and VE-cadherin, DII4 and Jag1, suggesting that leaders and followers cooperate via VEGF-activated Notch/Delta/Jagged and Cadherin signaling pathways[23].

In this study, we build an evolutionary game theory model to investigate the dynamics in the NSCLC collective invasion. In particular we focus on how the collaboration between leader and follower shape collective invasion and aim to find the interaction that can disrupt the collective invasion. The pairwise interactions between leader and follower cells are based on data from in vivo invasion assays.

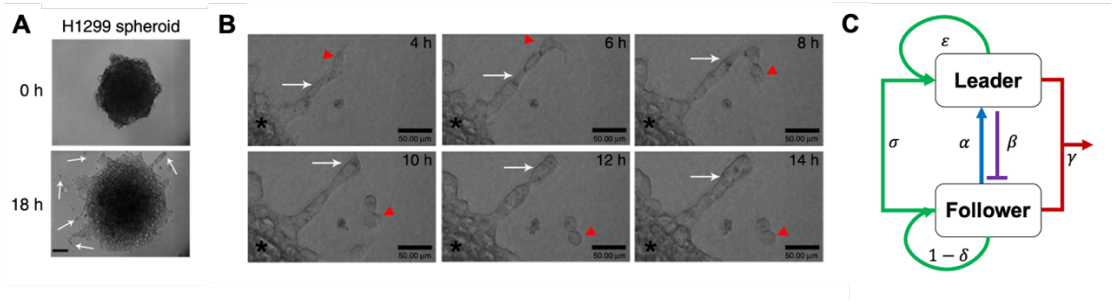

Figure 3-1 Leader and follower ecosystem in collective invasion
(A) H1299 spheroid embedded in collagen was imaged at 0h (top) and 18h (bottom) post embedding. Arrows, leader-follower invasive chains[23]. (B) Time lapse of H1299 spheroids imaged using live cell confocal imaging every 2h. Arrow, follower cells in invasive chains; red arrowhead, leader cells[23]. (C)Schematic of the pairwise interactions between leader, follower cells and the environment in collective invasion of our model. *(Reproduced with permission from Konen, J et al. Nat. Commun. 8, 1-15 2017)*

3.3 Methods

3.3.1 Evolutionary game theory model for collective invasion

Treating the collective invasion pack as an ecosystem, we analyze the dynamic evolution of a tumor consist of two subpopulation cancer cell phenotypes, leaders (L) and

followers (F) cells. Cell fitness is defined as the relative growth rate. Leader cells have proliferation defects, corresponding to a very low growth rate, $\varepsilon < 1$. For simplicity, we assume this growth rate is a constant, independent of the exact composition of the population and treatment conditions. Followers have a reference a growth rate of 1 and make up the majority of the population. They compete for space and resources with a competition strength δ. The follower cells support the growth of leader cells by secreting an undefined growth factor, which contributes to the leader's growth rate by α. The leader cells secrete a growth inhibitor that reduces the growth rate of the follower cells by β, at the same time collective invasion helps the followers to gain access to better growth environment, thus an improving their growth rate by γ[23,31]. To account for the observed plasticity between follower and leader cells, we include a conversion rate σ from follower cells to leader cells. Using the evolutionary game theory framework, these interactions between leader (L) and follower (F) cells can be described by the following payoff matrix[11,73], the parameters for which are listed in Table 1. Note that all the interaction parameters are non-dimensional and between 0 and 1.

$$P = \begin{matrix} \\ L \\ F \end{matrix} \begin{matrix} \begin{matrix} L & \quad F \end{matrix} \\ \begin{pmatrix} \varepsilon & \varepsilon + \alpha \\ 1 - \beta + \gamma & 1 - \delta \end{pmatrix} \end{matrix},$$

Table 3-1 Parameters Used for the Evolutionary Game Model

Parameters	Biological Interpretation	Value (Range)	References
L	Leader Cells		
F	Follower Cells		
x_i	Fraction of i^{th} Phenotype	$[0,1]$	
f_i	Fitness of i^{th} Phenotype	$[0,1]$	
ϵ	Relative Proliferation Rate of Leader Cells	0.1	(Konen 2017)
α	Leaders' Fitness Gain Supported by Follower Cells	$[0,1]$	
β	Followers' Fitness Loss by Leader Cells' Secretion	$[0,1]$	
γ	Followers' Fitness Gain by Leader Cells' Migration	$[0,1]$	
δ	Competition within Follower Cells	$[0,1]$	
d	Drug-induced Death Rate	$[0,1]$	
K	Carrying Capacity of Tumor	10^9	(Xiaoqiang 2016)
σ	Conversion Rate from Follower to Leader Cells	$[0,1]$	

The proportions of leader and follower cells are $x(t)$ and $1-x(t)$. The dynamics of the tumor is described by the replicator equations

$$\frac{dx}{dt} = x(1-x)\big((A+B)x - A\big),$$

where

$$A = P_{11} - P_{01},$$

$$B = P_{00} - P_{10}.$$

The replicator equation has equilibria $x = 0$, $x = 1$ and $x^* = \frac{A}{A+B}$ when $\frac{A}{A+B} \in (0,1)$.

1. If $A > 0$ and $B < 0$, then $x = 0$ is a stable fixed point, the follower cells dominate over follower cells, which corresponds to Prisoner's Dilemma.
2. If $A < 0$ and $B > 0$, then $x = 1$ is a stable fixed point, the leader cells dominate over leader cells, which corresponds to Harmony Game.
3. If both $A, B > 0$, the game is defined as Stag Hunt. This is characterized by bistability, when both equilibria $x = 0$ and $x = 1$ are stable, while $x^* = \frac{A}{A+B}$ is unstable.
4. If both $A, B < 0$, the game is defined as Hawk-Dove game. The equilibria $x^* = \frac{A}{A+B}$ is stable, and $x = 0$ and $x = 1$ are unstable.

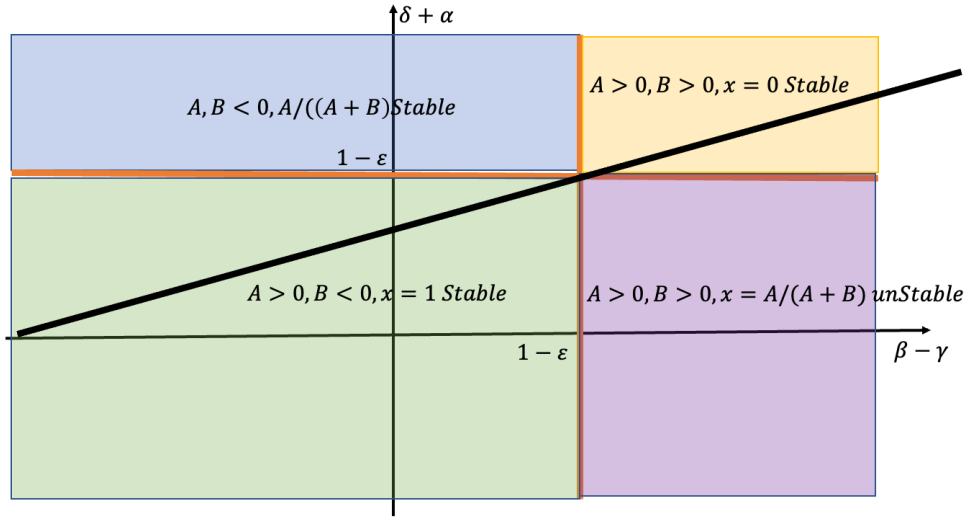

Figure 3-2 Schematic Diagram of Evolutionary Game Theory Model with Various Pairwise Interaction Intensities

In a well-mixed population, with fraction x_L of leader cells (L), the fitness functions of this game are given by

$$\begin{cases} f_L(x_L) = \varepsilon x_L + (\varepsilon + \alpha)x_F \\ f_F(x_F) = (1 - \beta + \gamma)x_L + (1 - \delta)x_F \end{cases}$$

The growth dynamics of leader and follower are characterized by

$$\frac{dN_L}{dt} = N_L f_L(x_L) + \sigma N_F$$

$$\frac{dN_F}{dt} = N_F f_F(x_F) - \sigma N_F$$

In particular, as leaders are the drivers of collective invasion, we introduce the fraction of leader cells and follower cells $(x_L,\ x_F)$ in tumor population

$$x_L = \frac{N_L}{N_L + N_F}, \qquad x_F = \frac{N_F}{N_L + N_F} = 1 - x_L$$

We simplify the equations (the so-called replicator equations with $N, x = x_L$ as variables) of the following system:

$$\frac{dN}{dt} = [f_L(x) - f_F(x)]Nx + f_F(x)N. \quad (1)$$

$$\frac{dx}{dt} = [f_L(x) - f_F(x)]x(1-x) \quad (2)$$

3.4 Results

3.4.1 Tumor growth and Leader-Follower Composition

To analyze the dynamics of the leader cells in the population, we investigate how the leader fractions and tumor size depend on the interaction parameters, including the pairwise interactions between leader and follower cells α, β and benefit due to improved environment for followers γ, and the follower growth competition δ. Starting with a strong competition within follower cells ($\delta = 0.8$), we see that with or without phenotypic conversion and regardless of the initial condition, the leader cell fraction arrives at a steady state (Figure 3-2 A). Not surprisingly, without follower to leader conversion, tumors without leaders initially remain without leaders over time (dashed blue line); with

phenotypic conversion from follower to leader (solid lines for $\sigma = 0.05$), the leader fraction within the tumor is higher than without phenotypic conversion (dashed lines for $\sigma = 0$). What is surprising is the overall growth rate (fitness) is higher when the leader fraction is higher (Figure 3-3B), which is counter-intuitive because the leaders have a much lower growth rate. The total tumor size data corroborate this finding, suggesting the phenotypic conversion from follower to leader cells significantly increases the overall tumor fitness through evolution.

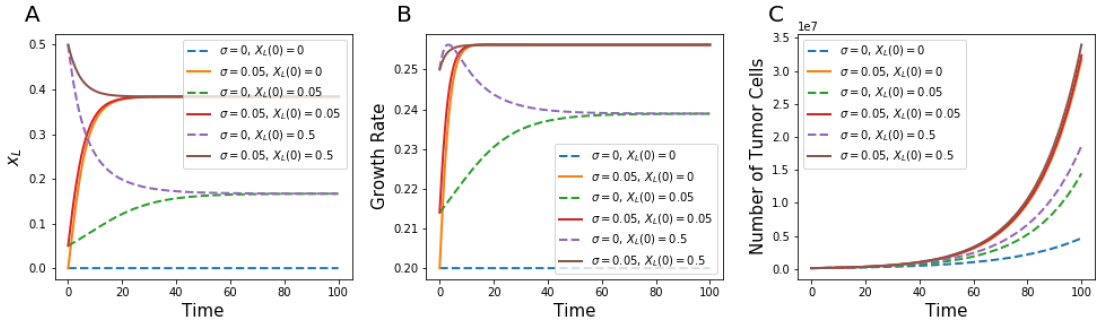

Figure 3-3 Tumor Dynamic of the Evolutionary Game Model I

Parameters: $\varepsilon = 0.1, \alpha = 0.2, \beta = 0.6, \gamma = 0.2, \delta = 0.8$. Comparison between phenotypical inconvertible (dashed lines) and convertible (solid lines) from follower to leader cells. (A) Leader cell fraction as a function of time arrives at a steady state from various initial conditions; without follower to leader conversion (dashed lines, $\sigma = 0$) and with follower to leader conversion (solid lines, $\sigma = 0.05$) (B) Overall relative growth rate f_N under various initial settings with (solid lines) and without (dashed lines) follower to leader conversion. (C) Tumor cell number dynamics with various initial settings. With the conversion possibility, the growth of the tumor is accelerated compared with no phenotypical switching.

To study how the cell-cell interactions affect the tumor growth, we change one variable at a time and fix the rest as the baseline parameters used in Figure 3-3. We focus on the disease burden (the total number of tumor cells N) and the metastatic potential (corresponding to the fraction of leader cells x_L). The tumor cell number (Figure 3-4A) shows that,

1. The stronger the competition between follower cells, the lower the long-term tumor burden (red line);

2. Increasing any of the other cell-cell interactions, including follower helping leader by growth factor (α, blue line) and leader inhibiting follower through growth inhibitor (β, orange line), and leader benefiting follower through invasion (γ, green line) leads to increased tumor burden;
3. Stronger follower to leader phenotypic conversion (σ, purple) also slightly increases the tumor burden.

Regarding the metastatic potential as measured by the leader cell fraction, it is expected that stronger follower helping leader (Figure 3-4B, blue line), leader inhibiting follower (orange), and follower to leader conversion (purple) would increase leader cell fraction. It is interesting that stronger benefit to the follower from collective invasion leads to lower leader fraction (green), as collective invasion allows more followers gain access to better growth environment and avoid competition within followers, and the consequential follower growth decreases the leader cell proportion.

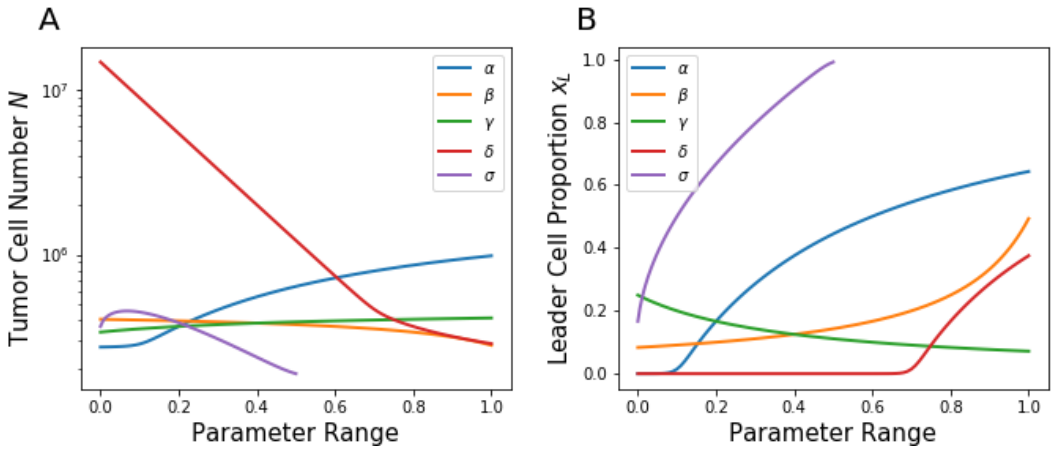

Figure 3-4 Dependence of the tumor burden as measured by the tumor cell number

(A) and the metastatic potential as measured by the leader cell proportion (B) on the cell-cell interactions, including follower benefiting leader growth via a growth factor (α, blue), and leader inhibiting follower growth via a growth inhibitor (β, orange), and collective invasion benefiting follower growth (γ, green), follower-follower growth competition (δ, red), and follower conversion to leader (σ, purple). The baseline parameters are $\varepsilon = 0.1, \alpha = 0.2, \beta = 0.6, \gamma = 0.2, \delta = 0.8$, and $\sigma = 0.05$. Only one parameter is varied at a time.

Not all interactions have the same scale of effect on the tumor growth (Figure 3-4A). For example, increasing follower competition, δ, has more dramatic effect on the tumor size than same amount of change in any other interactions (Fig 3-4A). Similarly, increasing the rate of conversion from follower to leader, σ, can increase the leader proportion much faster than the other parameter. To understand how different interactions, work together to shape the tumor growth and leader proportion, we analyzed the tumor growth dynamics in a multiple dimensional parameter space. With two parameters varied simultaneously (Fig 3-5, and Fig 3-9 – Fig 3-11), the results provide an alternative view of the tumor growth dynamics: in addition to what we already learned from Fig 3-4, we can compare how sensitively the growth dynamics depends on each of the interaction parameters.

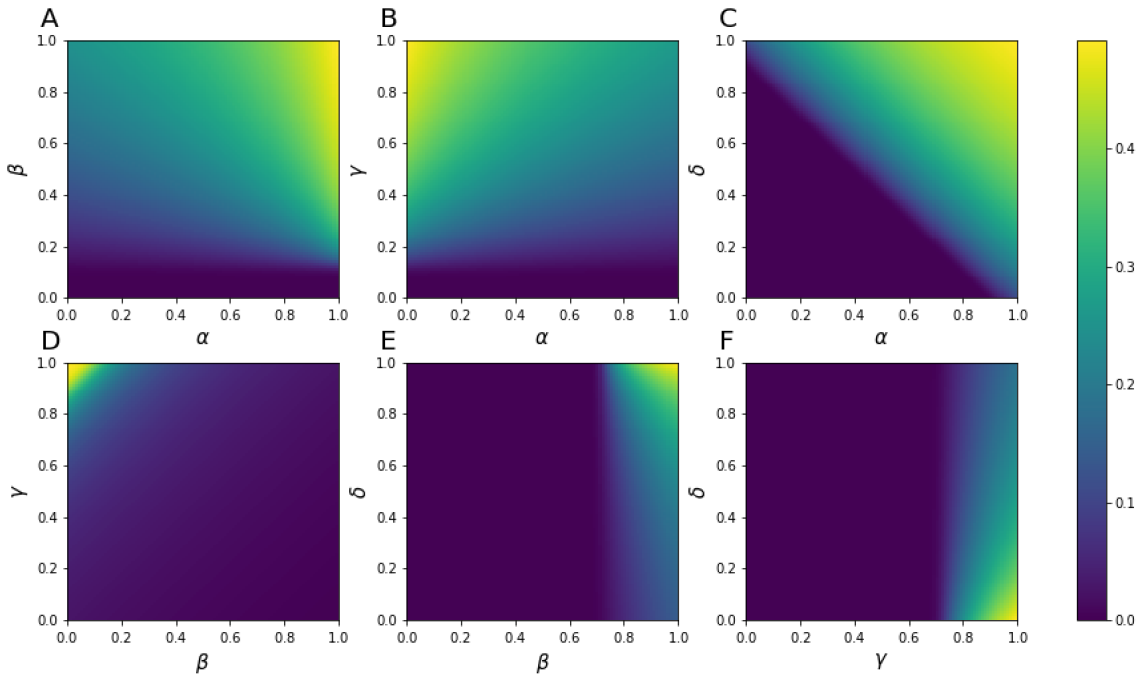

Figure 3-5 Coupled pairwise parameters influence the leader composition in the tumor I

Parameters: $\varepsilon = 0.1, \alpha = 0.2, \beta = 0.6, \gamma = 0.2, \delta = 0.8$ (two parameter changes per heatmap). (A-F). Leader Cell Composition without phenotypical switching from follower to leader cells. (See Fig 3.8 for Leader Cell Composition with phenotypical switching from follower to leader cells, Fig 3.8-3.10 for tumor cell numbers with and without convertibility)

3.4.2 Targeting Leader-Follower Interaction as A Novel Chemotherapy Strategy

The invasion assays of NSCLC spheroids *in vitro* revealed that the interactions between leaders and followers are mediated by molecular signals[23,31], we explore the idea of novel chemotherapies targeting these interactions. Here we ignore the emergence of the drug resistance for simplicity.

We use this evolutionary game theory framework to quantify the effects of novel chemotherapies targeting the following three interaction: inhibit follower proliferation or follower competition (F-F), promote leader inhibition towards follower proliferation (L-F), and inhibit follower-leader promotion (F-L). As we assume the growth rate of leaders is

low, we do not consider targeting leader cells proliferation, and consider the exponential growth as the baseline growth dynamics for leaders. (We explore an alternative logistic growth model in Supporting Information.)

The effect of treatment is added to the payoff matrix as a 'cost' d. For instance, when the drug reduces the proliferation rate of the follower cells, the term $1-\delta$ is replaced by $1-\delta-d$. The effects of these novel treatments on metastatic potential (leader proportion) and tumor burden (tumor fitness) show different trends for different treatments (Fig 3.5), but the trends remain the same with or without phenotypical conversion ($\sigma = 0$ solid lines, $\sigma = 0.05$ dashed lines).

1. ***Reduce Follower Proliferation (F-F):*** This treatment targeting the fast, proliferative subpopulation is widely used in clinically practice, such as cytotoxic chemotherapy agents. This strategy could efficiently reduce tumor growth. However, the undesirable side effect of this strategy is the increase in leader cells composition, higher potential for metastasis which is a major impediment for the cure (Fig 3-6, red lines).
2. ***Promote Leader-Follower Inhibition (L-F):*** This treatment is more effective in reducing tumor growth rate than the F-F strategy. But similarly, at the same time the cost is an even higher leader proportion than F-F, corresponding to higher metastatic risk (Fig 3-6, blue lines).
3. ***Inhibit Follower-Leader Promotion (F-L):*** This strategy is not as effective in reducing tumor growth rate as the other two cases, but its ability to drag down the leader proportion is unique. This strategy could reduce the risk of metastatic potential and meanwhile maintain a relative lower growth rate, suggesting a potentially optimal

intervention for long term tumor management.

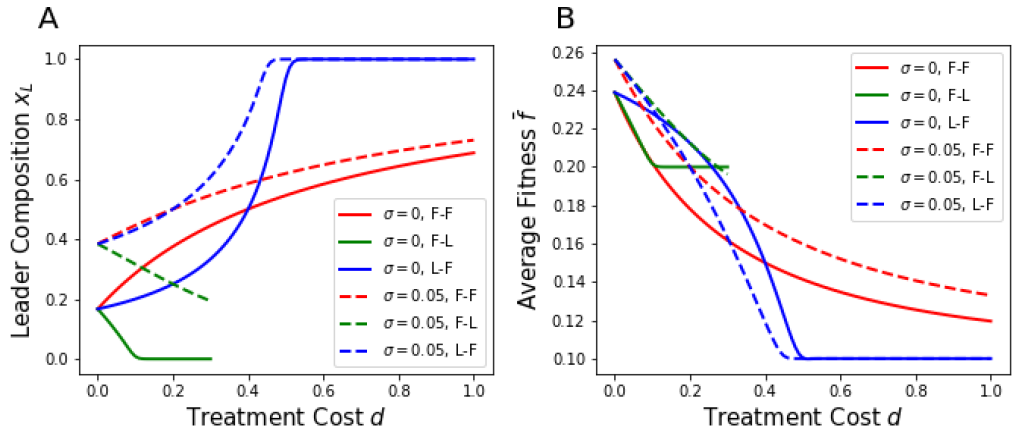

Figure 3-6 Treatment Cost and its Efficacy of the Evolutionary Game Model I
Parameters: $\varepsilon = 0.1, \alpha = 0.2, \beta = 0.6, \gamma = 0.2, \delta = 0.8$. Comparison between phenotypical inconvertible (solid lines) and convertible (dashed lines) from follower to leader cells. (A). Leader cells proportion evolution with various drug costs: the drug decreasing proliferation rate of follower cells (red lines); with the drug targeting follower-leader interactions (decrease follower promotes leader cells' proliferation (green lines); increase leader inhibits follower cells' fitness (blue lines)). (B). Average fitness of the tumor evolution with various drug costs.

Comparing convertible and inconvertible phenotypic switch cases, the tendencies are in consistence. However, as discussed in ***Leader-Follower Composition*** section, the possibility of phenotypic switch from follower to leader cells directly increase the leader cells proportion, and in F-F strategy increase the growth rate as well, while in other cases they're comparable. Comparison indicates the phonotypic plasticity could increase the robustness of the system under treatment selection.

Table 3-2 Three Protocols (Potential Targets) for Chemotherapy

Notation	Biological Interpretation	Effects
$F-F$	Reduce follower proliferation	Decrease tumor growth rate and increase leader proportion
$F-L$	Inhibit follower-to-leader promotion	Decrease Leader Proportion
$L-F$	Enhance leader-to-follower Inhibition	Decease tumor growth rate & increase leader proportion

3.4.3 Benefits of Drug Combination in Chemotherapy

Understanding how the interactions reshape the tumor evolution is crucial in designing optimal treatment strategies. Our model reveals the treatment principles for three types chemotherapy agents, targeting fast proliferative follower cells (F-F), inhibiting follower-to-leader cells promotion (F-L) and enhancing leader-to-follower cells inhibition (L-F), resulting in different effects for disease progression (summarized in Table 3-2). One example trajectory for treatment is depicted in Fig 3-7 (A-B), constant dosage to reduce fast-proliferative cells (F), results in phenotypic switching to highly migratory cells (L), which eventually increase the potential metastasis. An optimal strategy is to combine treatments and switch phenotypes during the chemotherapy, one trajectory is illustrated in Fig 3-7 (C-D). By switching chemotherapy agents, not only the total number of cells can be further reduced but also the proportion of the leader cells oscillates and result in lower risk of metastasis potential.

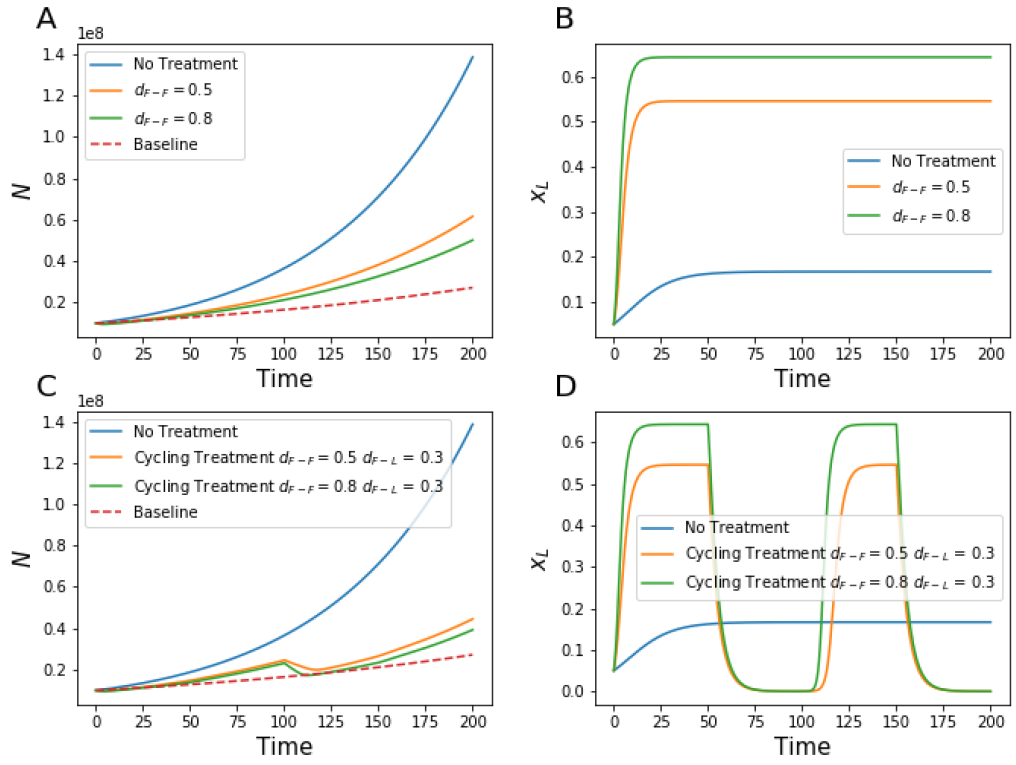

Figure 3-7 Evolutionary Dynamics of the Tumor under Different Treatment Protocols

Parameters: $\varepsilon = 0.1, \alpha = 0.2, \beta = 0.6\ \gamma = 0.2, \delta = 0.8$ (A)-(B). Tumor cell number and leader cell proportion under constant dosing with F-F treatment Strategy. (C)-(D). Tumor cell number and leader cell proportion under constant dosing cycling between F-F and F-L treatment strategies.

Switching phenotypes is one of an efficient strategies in cancer treatment to delay the emergence of drug resistance[22,74,75]. Our model suggests alternation of the phenotypes by targeting different pairwise interactions is also beneficial in lowering metastatic potential and disease burden. One of the example trajectories in Fig 3-8 is by switching strategies between F-F and F-L. Under the intensive chemotherapy targeting fast proliferative follower cells (F-F), the amount of follower cells decreases tremendously, meanwhile release the competition within the tumor. Therefore, the leader cells proportion will increase accordingly resulting higher risk of metastasis. The proper schedule switching treatment protocols to inhibit the promotion of follower cells

to leader cells' growth could induce competition between leader and follower cells and result in the decrease of leader cells which compromising the side effect of the previous treatment protocol (F-F). Comparing with the constant dosage treatment, the effect of the sequential drug switching could not only significantly reduce the leader cells proportion as discussed, but also exceed in reducing total tumor cells. This result may shine light in clinical practices.

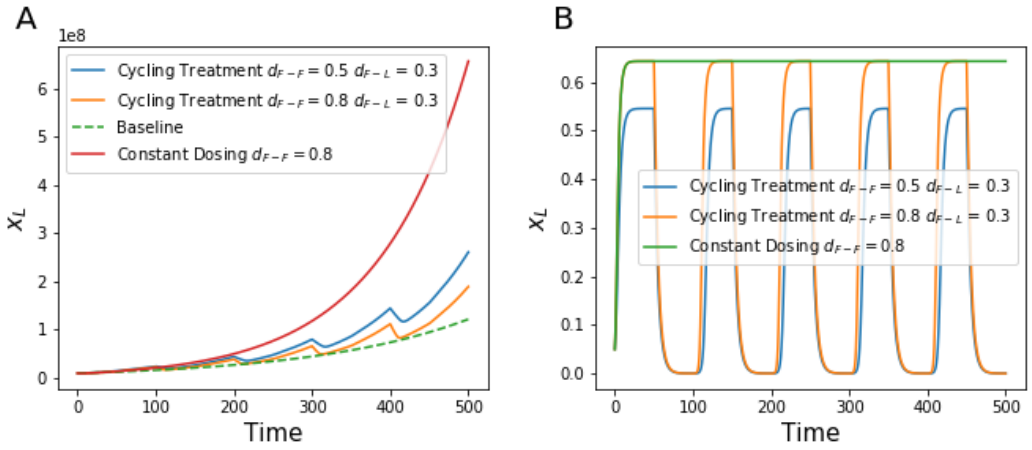

Figure 3-8 Evolutionary Dynamics of the Tumor under Different Treatment Protocols II

Parameters: $\varepsilon = 0.1, \alpha = 0.2, \beta = 0.6\ \gamma = 0.2, \delta = 0.8$ (A)-(B). Tumor cell number and leader cell proportion under constant dosing with F-F treatment Strategy

3.5 Discussion

In this study, we have developed a mathematical model to quantitatively analyze the proportions of two distinct phenotype, highly migratory leader cells (L) and fast proliferative follower cells (F). Corresponding to experimental observations[23,27] in collective invasion behaviors, the existence of leader and follower cells are confirmed in NSCLC cell line[23] and the pairwise interactions[31] are studied in order to characterize various collective situations.

Our model provides a theoretical testbed for exploring the chemotherapy schedule design and chemo-agents selection. The distinct interactions terms in the payoff matrix originated from leader-follower signals may suggests new drug targets for the treatments which reduces tumor burden as well as lower the metastatic risk.

3.6 Conclusion

Collective cancer invasion, where cells invade into peritumoral stroma as a cohesive and polarized mass maintaining cell-cell contacts, is shown to associate with better metastatic success and poor patient outcome. Even though we have identified distinct phenotypes in the collective invasion pack, the interactions between the phenotypes and between cells and the microenvironment have not been well understood. We use a game theory framework to decipher the roles of pairwise interactions in leader-follower collective invasion and analyze the dynamics of the system under various interaction intensities. These results suggest novel targets or treatment strategies to reduce tumor burden as well as lower metastatic risks.

In this study, we established an evolutionary game theory framework to describe the complex ecosystem of NSCLC collective invasion. Two distinct phenotypes, highly migratory leader cells (L) and fast proliferative follower cells (F) are critical in the dynamics of the tumor evolution. We analysis how the intensity of pairwise interactions between L and F influences the dynamics of the tumor growth population. Using our model, we could simulate how phenotypes contribute to tumor growth and may lead to different metastatic potentials. Based on our model, three potential treatment protocols

(F-F, F-L and L-F) are proposed by targeting different pairwise interactions between phenotypes. Additionally, we can observe that switching treatment protocols influences the tumor growth remarkably. This may imply novel targets in clinical practice which reduces tumor burden as well as lower the metastatic risks.

3.7 Supporting Information

3.7.1 Sensitivity of Pairwise Interactions to Collective Invasion Dynamics

To understand how different interactions, work together to shape the tumor growth and leader proportion, we analyzed the tumor growth dynamics in a multiple dimensional parameter space. With two parameters varied simultaneously (Fig 3-9 to Fig 3-11), the results provide an alternative view of the tumor growth dynamics: in addition to what we already learned from Fig 3-4, we can compare how sensitively the growth dynamics depends on each of the interaction parameters.

Fig 3-9 illustrates the influences of coupled parameters of the evolutionary game model with fixed parameters ($\varepsilon = 0.1, \alpha = 0.2, \beta = 0.6, \gamma = 0.2, \delta = 0.8$) with a phenotypic conversion rate $\sigma = 0.05$. When compared with Fig 3-5 (same parameter but without a mechanism for phenotypic conversion), the ability of the phenotypic conversion can increase the proportion of leader cells in general. The agent-based model in chapter 2 reveals the importance of leader and follower coexistence contributing to collective cancer invasion process. The phenotypic conversion is a robust mechanism to promote collective invasion.

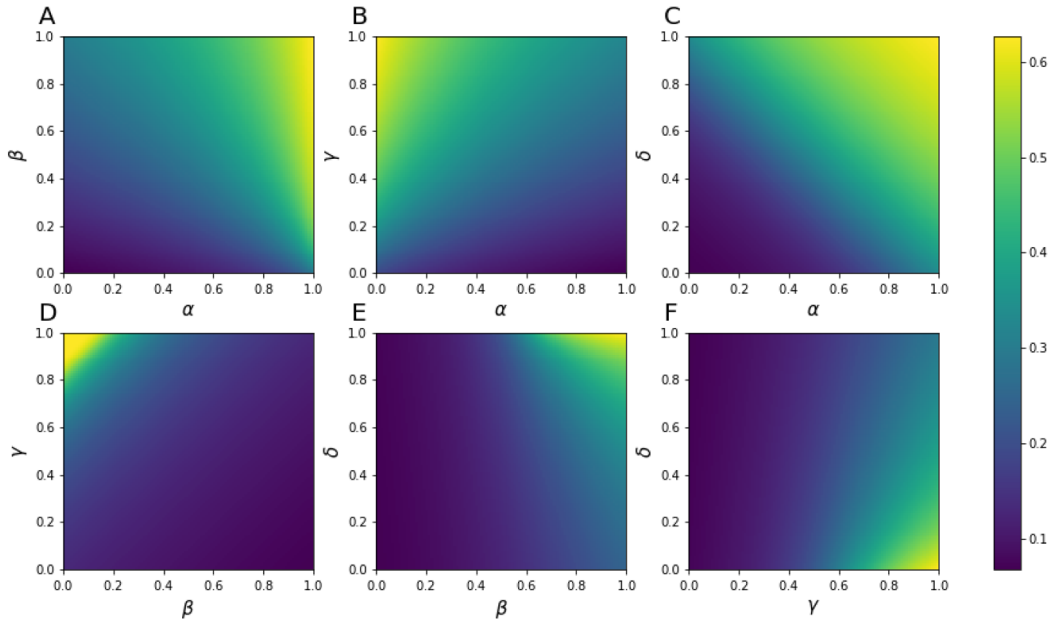

Figure 3-9 Influences of coupled parameters of the Evolutionary Game Model II
Parameters: $\varepsilon = 0.1, \alpha = 0.2, \beta = 0.6, \gamma = 0.2, \delta = 0.8$ (two parameter changes per heatmap). (A-F). Leader Cell Composition with phenotypical switching $\sigma = 0.05$ from follower to leader cells

Fig 3-10 and Fig 3-11 illustrate the influences of coupled parameters of the evolutionary game model with fixed parameters ($\varepsilon = 0.1, \alpha = 0.2, \beta = 0.6, \gamma = 0.2, \delta = 0.8$) without and with a phenotypic conversion rate $\sigma = 0.05$ in terms of total tumor cells. The ability of the phenotypic conversion cannot significantly increase the overall tumor proliferation. However, Fig 3-5 and Fig 3-9 demonstrate, enable phenotypic conversion from follower cells to leader cells can significantly change the intratumor heterogeneity (tumor composition). These results suggest that even when the disease burden is the similar, the phenotypic intratumor heterogeneity can alter the dynamics of the tumor: the metastasis potential is different.

The mechanism of the phenotypic conversion from follower cells to leader cells is a critical mechanism to maintain a high intratumor heterogeneity in terms of metastasis.

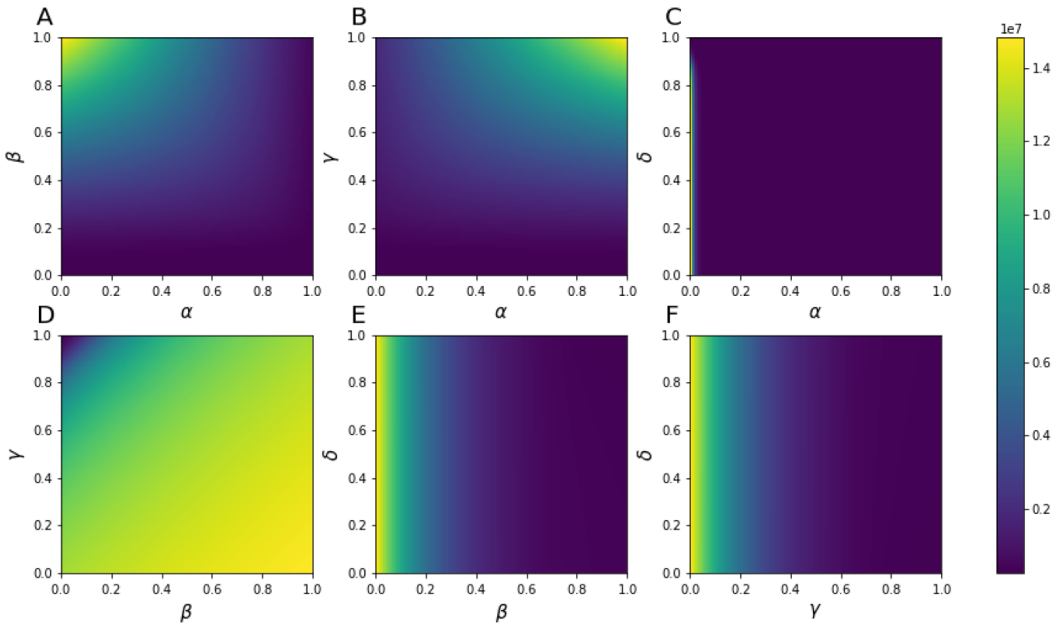

Figure 3-10 Influences of coupled parameters of the Evolutionary Game Model III
Parameters $\varepsilon = 0.1, \alpha = 0.2, \beta = 0.6, \gamma = 0.2, \delta = 0.8$ (two parameter changes per heatmap). (A-F). Tumor Cell Number at the end of simulation without convertibility.

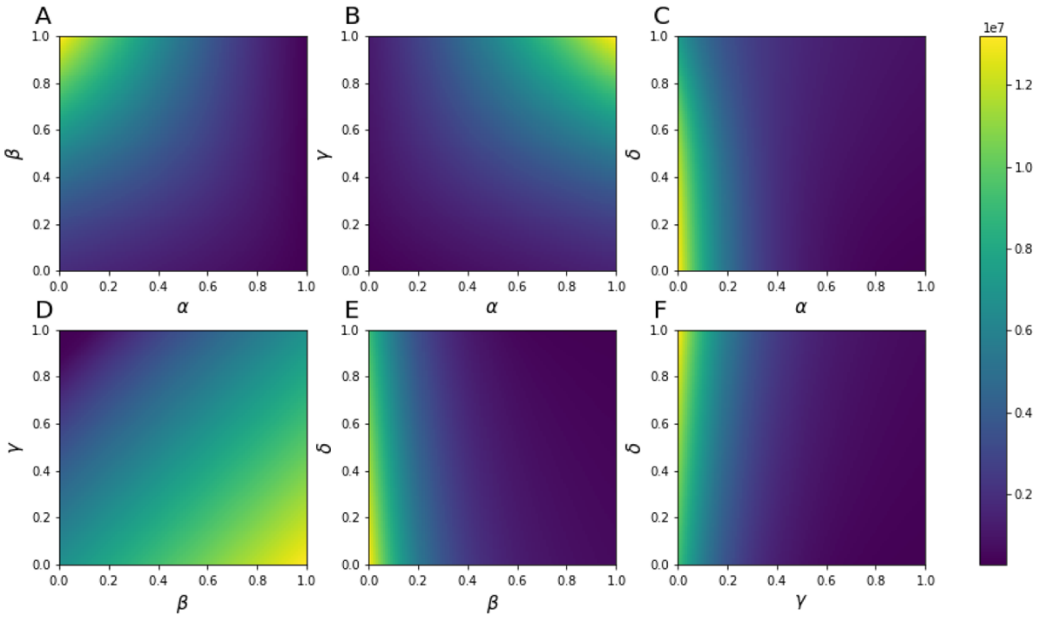

Figure 3-11 Influences of coupled parameters of the Evolutionary Game Model IV
Parameters $\varepsilon = 0.1, \alpha = 0.2, \beta = 0.6, \gamma = 0.2, \delta = 0.8$ (two parameter changes per heatmap). (A-F). Tumor Cell Number at the end of simulation with convertibility $\sigma = 0.05$

3.7.2 Stability Analysis

In the discussion above, we assume an unbounded exponential growth dynamic of the tumor, the competition within subpopulation δ could only reduce the growth rate and doesn't halt the growth. More realistically, we consider a modification to our model, logistic growth model with carrying capacity $K \sim 10^9$ and equal competition between two phenotypes. The evolutionary game model with the same payoff matrix could be modified as:

$$\frac{dN_L}{dt} = N_L f_L(x_L)\left(1 - \frac{N_L + N_F}{K}\right) + \sigma N_F$$

$$\frac{dN_F}{dt} = N_F f_F(x_F)\left(1 - \frac{N_L + N_F}{K}\right) - \sigma N_F$$

Therefore, we can obtain modified replicator equations ($N, x = x_L$) if no conversion is considered:

$$\frac{dN}{dt} = [f_L(x) - f_F(x)]Nx\left(1 - \frac{N}{K}\right) + f_F(x)N\left(1 - \frac{N}{K}\right)$$

$$\frac{dx}{dt} = [f_L(x) - f_F(x)]x(1-x)\left(1 - \frac{N}{K}\right)$$

The fixed points of the system can be derived by solving

$$\frac{dN}{dt} = [f_L(x) - f_F(x)]Nx\left(1 - \frac{N}{K}\right) + f_F(x)N\left(1 - \frac{N}{K}\right) = 0$$

$$\frac{dx}{dt} = [f_L(x) - f_F(x)]x(1-x)\left(1 - \frac{N}{K}\right) = 0$$

i. $(x_1, N_1) = (0, 0)$ with corresponding eigen values $\lambda_1 = f_F(0) = 1 - \delta$ and $\lambda_2 = f_L(0) - f_F(0)$. We assume the tumor cells have a positive net growth rate for both cell types and all $x \in [0,1]$, therefore $\lambda_1 > 0$. This fixed point is unstable;

ii. $(x_2, N_2) = (1, 0)$ with corresponding eigen values $\lambda_1 = f_F(1) = 1 - \beta + \gamma$ and $\lambda_2 = f_L(1) - f_F(1)$. We assume the tumor cells have a positive net growth rate for both cell types and all $x \in [0,1]$, therefore $\lambda_1 > 0$. This fixed point is unstable;

iii. $(x_3, N_3) = (0, K)$ with corresponding eigen values $\lambda_1 = f_F(0) = (1 - \delta)$ and $\lambda_2 = 0$. We assume the tumor cells have a positive net growth rate for both cell types and all $x \in [0,1]$, therefore $\lambda_1 > 0$. This fixed point is unstable;

iv. $(x_4, N_4) = (1, K)$ with corresponding eigen values $\lambda_1 = f_L(1) = \varepsilon$ and $\lambda_2 = 0$. We assume the tumor cells have a positive net growth rate for both cell types and all $x \in [0,1]$, therefore $\lambda_1 > 0$. This fixed point is unstable;

The stable steady state is (x_{L0}, K), where x_{L0} is determined by the payoff matrix. Fig 11 demonstrate the stability of the exponential evolutionary game model (Fig 3-12A and Fig 3-12C) and logistic evolutionary game model (Fig 3-12B and Fig 3-12D). For exponential model, there exist a stable steady $x_{L0} = x_0 \in (0,1)$ and unstable ($x_{L0} = 0$ and $x_{L0} = 1$) for inconvertible case and when the conversion is allowed, the stable steady state x_0 increase while unstable $x_{L0} = 0$ disappears and leaving $x_{L0} = 1$ as the only unstable steady fixed point. Similar to the exponential growth model, with phenotypic conversion, the system tends to evolve to the $(1, K)$, the only stable steady states shown in Fig 3-12.

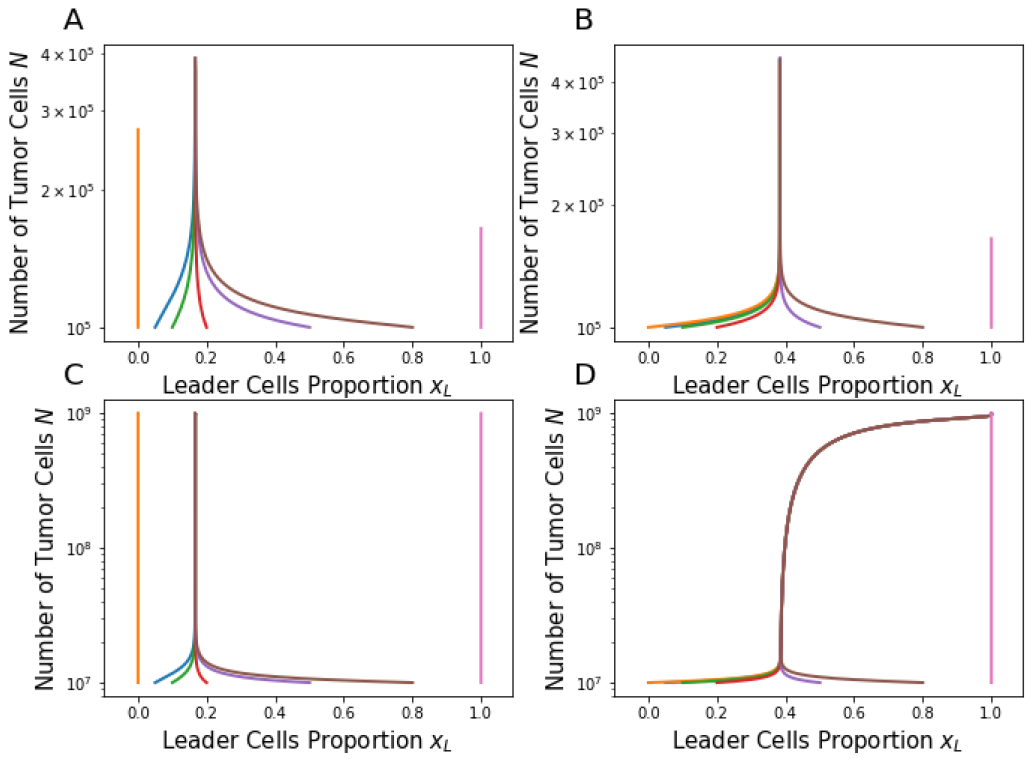

Figure 3-12 Phase Diagram of the Evolutionary Game Model

Parameters: $\varepsilon = 0.1, \alpha = 0.2, \beta = 0.6, \gamma = 0.2, \delta = 0.8$. Comparison between phenotypical inconvertible (A & C) and convertible (B & D) from follower to leader cells. Comparison between unbounded exponential growth (A & B) and logistic growth with carrying capacity $\mathrm{K} = 10^9$ (C & D).

4 How Allee Effect Improves the Probability of Tumor Eradication in Response to Chemotherapy

4.1 Abstract

One of the major impediments to successful cancer treatment is the emergence of drug resistance, which has led to prolonged tumor control as the treatment goal instead of tumor eradication. Recent preclinical models and in vitro experiments indicate that tumor growth rate increases with cell numbers at low cell densities, implying an Allee effect in tumor growth. Here, we propose a mathematical tumor growth model incorporating the Allee effect and drug resistance. We vary the effective chemotherapy dosage, resistant cell composition, tumor size at the start of treatment, and the Allee threshold to determine the treatment outcomes. These results offer optimal treatment designs based on personal treatment goals, whether that is prolonged tumor control with low dosage and low treatment side-effects, or tumor eradication using large dosage and possible serious side effects. These results suggest the reason combination chemotherapies can improve the probability of tumor eradication is because they reduce the resistant colony fraction from the start of treatment. Furthermore, we propose a new management strategy for patients with tumor numbers below the detection threshold after therapy (disease free): a second-strike consolidation treatment with a different chemo-agent. This strategy will decrease the chance of recurrence and increase the possibility of a complete cure.

4.2 Introduction

Cancer is an evolutionary disease which exhibits genomic[52] and phenotypic[76] heterogeneity, this phenomenon is of critical significance in tumor initiation, progression, metastasis, therapeutic response and recurrence[20,23,77,78]. One of the obstacles for the cure of the cancer is the emergence of drug resistance. Drug-induced resistance together with high intratumor heterogeneity serves as a barrier for successful treatment, which means for a large tumor, for any given drugs, it's likely there exists a small resistant population within the tumor. These cells could survive under chemotherapy and repopulate leading to treatment failure. Intensive theoretical studies explore optimal therapy strategies[17,20–22] to prolong tumor control with integration of phenotypic intratumor heterogeneity evolution under various assumptions, whose goals are prolong tumor control instead of tumor eradication. Some of the key factors leading to success treatments are understanding the dynamics of the tumor growth and the evolution of intratumor heterogeneity.

The classical models describing tumor growth are usually formulated in terms of differential equations that relates the growth rate of the tumor to its current state and increase its complexity from simple one-parameter exponential growth to advanced models considering tumor heterogeneity[44]. The exponential model captures the tumor growth pattern by a constant growth rate r and assuming unconstrained cell divisions, therefore it's unrealistic to explain tumor growth in the long term. Logistic model modifies the intrinsic growth rate with a linear decrease on the current state and limiting

the total population size to carrying capacity K and widely applied to various biological systems. Similarly, Gompertz model captures the decrease growth rate over time and was applied to describe tumor growth[43] and become a popular model[44]. These models and their derivatives focus on a high tumor cell density.

At a low tumor cell density, the Allee effect should be considered. Allee effect[79] is introduced as a phenomenon in ecology, where the growth rate is dependent on the population size. Individuals require assistance and cooperate to persist and increase the survival rate where there're fewer individuals. This effect is known as Allee effect in ecology[80] and arises due to cooperative interactions, such as cooperative growth, predation[39] and modification of the environment[64,80].

The mathematical formulation can be divided into strong and weak Allee effect. Strong Allee effect could result in a negative growth rate at very low population density, however weak Allee effect always guarantees a positive growth rate.

1. Strong Allee Effect[6]

$$\frac{dN}{dt} = rN(1 - \frac{A}{N})$$

2. Weak Allee Effect[81]

$$\frac{dN}{dt} = rN(1 - \frac{A + \tau}{N + \tau})$$

In tumor growth dynamics research field, recent preclinical mouse model[82] and in vitro experiments[39] suggests the growth rate scales with population size at low cancer cell densities.

Experiments cultivating breast cancer cell at extreme low density in a controlled in vitro setting deviates from exponential growth, suggesting an Allee effect at low cell

density[81]. The longitudinal tumor growth data is fitted to an Allee effect formulation and indicates cooperation among tumor cells at low tumor cell density.

Pre-clinical data for the recurrence rate of glioblastoma after resection also suggests an Allee effect[65]. In glioblastoma cell proliferation rate increases as the density at small cell number regime, which suggest the cooperation among tumor cells plays a significant role in determining the glioblastoma recurrence time.

Therefore, understanding tumor growth dynamics at low cell numbers is essential to develop optimal clinical strategies for cancer treatment. The consequences of low cell density growth dynamics including tumor initiation, metastasis, recurrence etc. are of significant clinical importance. Integrated with tumor evolution dynamics, the treatment outcome could be improved and lead to better cure rate.

4.3 Model

Here we introduce a general mathematical modeling framework to describe the tumor dynamics at a cellular population level and evolution of drug resistance during treatment. We consider the tumor to be composed of two phenotypes regards of chemotherapy, sensitive (S) and resistant cells (R). Sensitive (wildtype) cells are fully susceptible to the treatment. We use a system of two ordinary differential equations to describe the dynamics between S and R subpopulations with all non-negative parameters:

$$\frac{dS}{dt} = r_0\left(1 - \frac{A}{S+R}\right)\left(1 - \frac{S+R}{K}\right)S - \big(u + \alpha U(t)\big)S - dU(t)S - d_0 S$$

$$\frac{dR}{dt} = r_R\left(1 - \frac{A}{S+R}\right)\left(1 - \frac{S+R}{K}\right)R + \big(u + \alpha U(t)\big)S - d_0 R$$

Table 4-1 Parameters Used for the Model with Allee Effect

Parameters	Biological Interpretation	Value (Range)	References
$S(t)$	**Sensitive Population**		
$R(t)$	**Resistant Population**		
$U(t)$	**Treatment Dosing**		
A	**Allee Effect Threshold ($A << K$)**	$[10^2, 10^5]$	(Kaitlyn, 2019)
r_0	**Intrinsic Growth Rate of Sensitive Population**	$0.13/Day$	(Bozic 2013)
r_R	**Intrinsic Growth Rate of Resistant Population**	$0.10/Day$	(Xiaoqiang 2016)
d_0	**Intrinsic Death Rate of Tumor Cells**	$0.09/Day$	(Bozic 2013)
d	**Drug-induced Death Rate of Sensitive Population**	$[0, 0.3]$	
α	**Drug-induced Resistance Rate**	$[10^{-5}, 10^{-1}]$	(Greene 2019)
u	**Spontaneous Mutation Rate**	10^{-6}	
K	**Carrying Capacity of Tumor**	10^9	(Xiaoqiang 2016)

4.3.1 Tumor Growth Dynamics

In the absence of treatment, we assume the tumor follows a logistic growth rule, with each subpopulation contributing equally to the intratumor competition[26]. Each phenotype possesses different intrinsic growth rates, supported by experimental evidence, we make assumption that $0 \leq r_R < r_0$, where resistant subpopulation grows slower than the sensitive cells. Recent preclinical and clinical observations of tumor initiation and recurrence indicate the presence of tumor growth kinetics in which growth

rates scale positively with cell numbers, suggesting an Allee effect at the regime of low number of tumor cells[39]. In vivo, some confounding factors, such as tumor microenvironments and immune responses may cause and mask the deviation from exponential growth dynamics at a low cell population level. Therefore, we assume a strong Allee effect with a critical threshold A to model the tumor growth dynamics at low tumor cell population level.

4.3.2 Drug Resistance Evolution

The transition from the wildtype to the resistant is described in term of $(u + \alpha U(t))S$, which comprises spontaneous resistance evolution and drug-induced resistance transitions[21]. Mathematically, uS, independent of the treatment, is the net result of mutations; $\alpha U(t)S$, dependent on treatment schedule and dosing $U(t)$, describes the linear effect of treatment promoting the resistant phenotype.

4.3.3 Drug Efficacy

We model the effects of the treatment by log-kill hypothesis[83], which assumes regardless of tumor size, a given dosage of chemotherapy agent eliminates the same fraction of tumor cells. By simplification, we assume the chemotherapy agents are completely ineffective against resistant subpopulation. Finally, we note that the effective drug concentration $U(t)$ could be as a control input. For simplicity, we assume it is directly proportional to the applied drug concentration, however, pharmacokinetics considerations could be incorporated to more accurate form of mathematical models in vitro or in vivo.

4.4 Results

4.4.1 Growth Rate per Capita

We denote the tumor volume at time t by $N(t)$:

$$N(t) \coloneqq S(t) + R(t)$$

The growth rate per capita is defined as

$$\sigma(N) \coloneqq \frac{1}{N}\frac{dN}{dt}$$

The composition of resistant tumor cells is $x(t) = \frac{S(t)}{N(t)}$, which influences the overall tumor growth rate $\sigma(N) \coloneqq \frac{1}{N}\frac{dN}{dt} = \left(1 - \frac{A}{N}\right)\left(1 - \frac{N}{K}\right)\left(r_R + (r_0 - r_R)x(t)\right) - dU(t)x(t) - d_0$. Fig 4.1 shows the growth rate per capita of the tumor with different resistance compositions under our model assumptions. In the regime of low tumor cells, the growth rate increases as the tumor grows. This is the result of Allee effect of the model. At high tumor cell population level, due to the limited resources such as space and nutrients, the growth is slowing down. While, within a large range of number of tumor cells, the growth dynamics approximately follow exponential growth. When the composition of the resistance is fixed, the overall growth rate is a constant. Thus, at a relatively low tumor cell population level, we can ignore the linear decrease of tumor growth rate effect due to the carrying capacity.

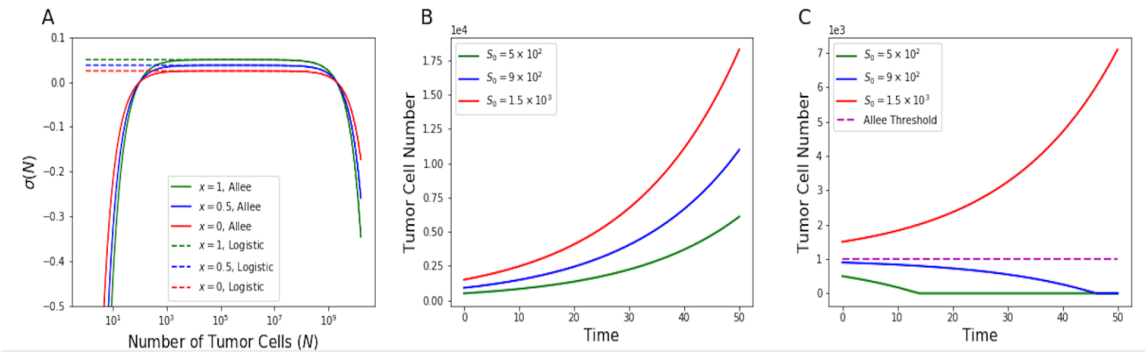

Figure 4-1 Tumor Growth Dynamics with/without Considering Strong Allee Effect
(A). Growth rate per capita of the tumor with various resistant tumor cells compositions by the model. The growth rate per capita scales positively with cell numbers at a low cell population level and decreases at a high tumor cell number (around the order of carrying capacity). Within the large regime of tumor cell number, the growth rate per capita maintains a constant when the resistant composition is fixed. (B). Dynamics of exponential tumor growth model, the tumor will eventually become prosperous regardless of the initial conditions; (C). Dynamics of tumor growth model considering Allee effect, the tumor growth pattern depends on initial conditions: Allee threshold acts as a critical point of the growth.

4.4.2 Treatment Protocol

To quantify the effects of Allee effect in the treatment, the treatment protocol is specified as Fig 4.2 below. We assume the initial tumor cell number is N_0, the tumor cell number progresses untreated until a certain disease burden N_0 at diagnosis or after the radical surgery.

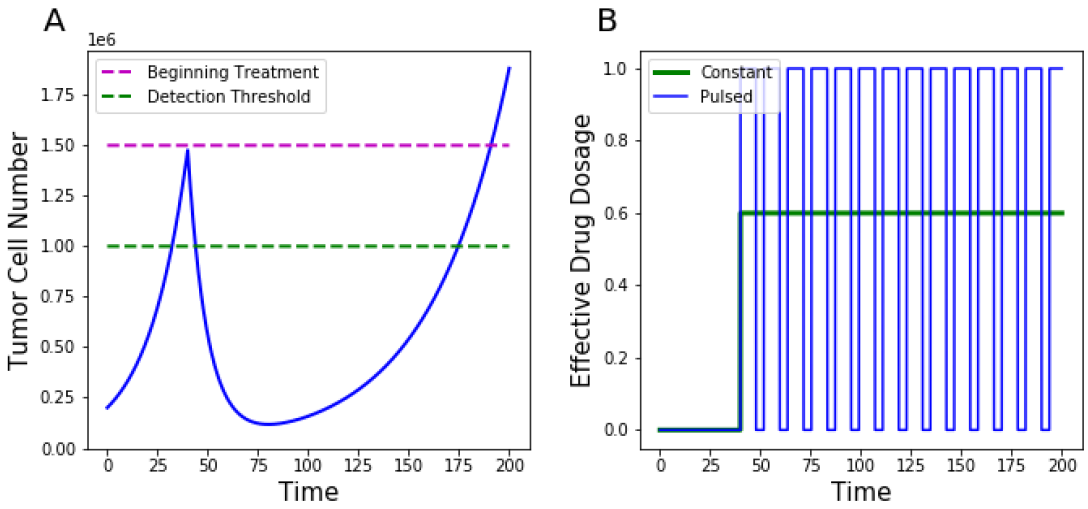

Figure 4-2 Schematic of tumor dynamics under two treatment regimes
(A) Tumor number in response to treatment initiated at diagnosis. Treatment is begun at this time and continues until the tumor reaches a critical size. (B) Illustrative constant dosage and pulsed treatment, both initiated at diagnosis.

We assume that the chemotherapy initiated at a relative low number of tumor cell number.

$$N_0 = S(0) = 10^5, \quad R(0) = 0$$

The treatment protocols are constant with different dosing used for chemotherapy $U(t) = C$. The dynamics of the treatment is different, because of the Allee effect. Fig 4.3 (A) demonstrate the treatment protocols: depending on the estimation of resistant composition and initial disease burden where chemotherapy is applied, the goals for the treatment is significantly different: some situations, the seek for tumor eradication is preferred, while in other cases, the management to prolong the tumor control is preferred. Our model demonstrates the assessment criterions from a theoretical framework standpoint and may shine light on the implications with clinically relevance. Fig 4.3 (B) shows the dynamics of system and evolution of phenotypic resistance. Initiated with the same amount wild-type sensitive tumor cells, the high

dosage treatment reduces the disease burden rapidly and approaches the order of Allee threshold, where the Allee effect dominates rather than the emergence and repopulation of the resistant colonies leaving the chemotherapy agents ineffective. Therefore, the tumor is eliminated. However, for the low dosage treatment, the emergence of the resistant colonies delays compared with the high dosage protocol. However, before the system decreases to the order of Allee threshold, the resistant colony dominates and causes the relapse in the future.

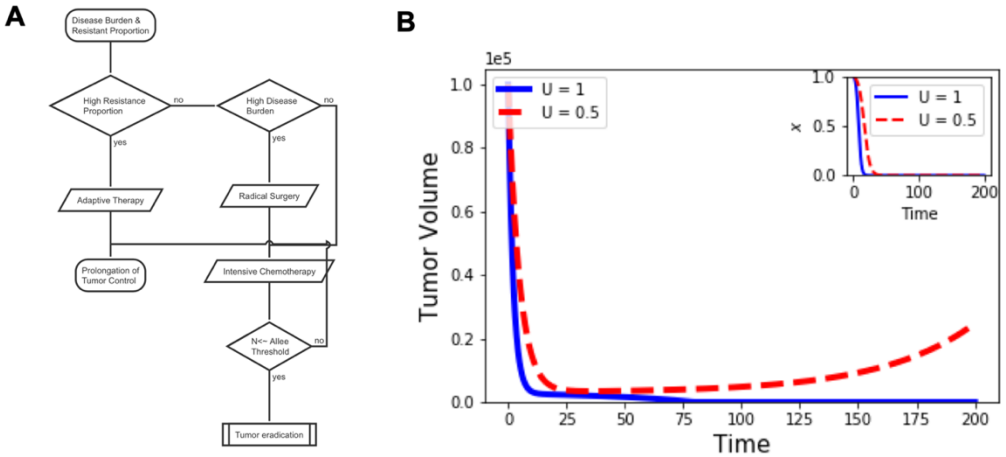

Figure 4-3 Schematic Diagram of the Treatment Strategy Selection and Tumor Growth Dynamics

(A)Flowchart of the treatment protocol for the model, from the model framework, the key factors for assessment are resistant composition and disease burden when chemotherapy is applied; (B)Tumor dynamics under two treatment protocols. Initiated with $S(0) = 10^5, R(0) = 0$ and $A = 10^3$. The high dosage treatment $U(t) = 1$ (solid blue lines) could reduce the disease burden and eliminate the tumor even with earlier resistant colonies emerge. The low dosage treatment $U(t) = 0.5$ (dashed red lines) could reduce the disease burden initially, because of the emergence of the resistant tumorous cells, the tumor cells repopulate and lead to relapse in the future if there's no changes in treatment protocol.

4.4.3 Effect of Allee Threshold Versus Effective Drug Concentration

The core of the successful treatment of our model is the Allee effect, which is determined by Allee threshold A. To quantitively demonstrate the role that Allee effect plays in the elimination of tumor cells, we consider multiple effective drug

concentrations with a constant dosage with a long enough treatment protocol (reaching the steady states of the system). Initiated with $N_0 = S(0) = 10^5$ and $R(0) = 0$, with various Allee thresholds and effective drug concentrations, we evaluate the evolutions of the system. The results are summarized in Fig 4.4. By examining Fig 4.4, three behaviors of the system is observed: when the effective drug concentration is at an extremely low level, the wildtype dominates the tumor composition and reaches to carrying capacity (yellow region in Fig 4.4); with the increase of the effective drug concentration, the resistant colonies takes over the wildtype and repopulate to its carrying capacity (green region in Fig 4.4); with sufficient drug and a decent Allee threshold A, the tumor could be eliminated and achieve a complete cure (dark blue region in Fig 4.4).

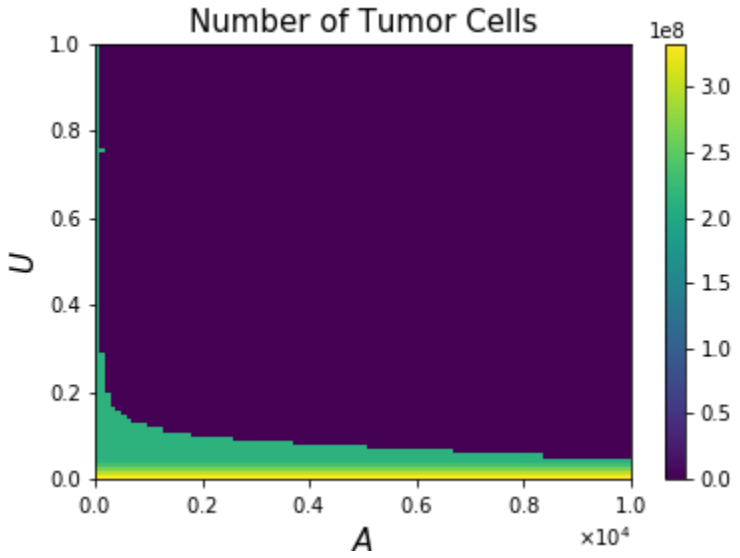

Figure 4-4 Tumor dynamics under multiple effective drug concentrations and Allee thresholds

The treatment starts with $S(0) = 10^5, R(0) = 0$. With an extremely low drug dosage, the wildtype dominates the tumor dynamics (yellow region); with the increase of the dosage, the resistant phenotype takes over the composition of the tumor cell population (green region); with sufficient dosage and Allee threshold, the tumor cells could be eliminated, resulting in a complete cure of the cancer (dark blue region).

4.4.4 Disease Burden Versus Drug Concentration

The design of an effective chemotherapy requires comprehensive considerations of the patients, key factors including tumor size, composition of resistant phenotypes, immune responses, drug tolerance greatly influence the prognosis. To qualitatively demonstrate the influences of the tumor size to the prognosis, we calculate the steady states with various dosage and initial disease tumor cell number. We assume no resistant phenotype exists initially. Intuitively, with the increase in tumor size, the probability of tumor elimination is negatively scaled. Fig 4.5 (A) confirms this trend: for a given initial tumor size, there exists a threshold of effective drug concentration for tumor elimination, this threshold positively scales with the initial tumor size. Similarly, three different colored regions represent different tumor dynamics as in Fig 4.4.

4.4.5 Drug Resistance Versus Drug Concentration

Cancer is an evolutionary disease, typically when the treatment is initiated, the resistant phenotype already exists[20]. The responses to the chemotherapy agents initially greatly alter the outcomes of the patients' survival[73,84,85]. We feed the system with different composition of resistant phenotypes of the tumor, 0%, $1\%, 5\%$ and 10% at the beginning of the treatment. Fig 4.5 qualitatively demonstrates the influences of the resistance to the prognosis. As the percentage of resistant cells increases, the dosage of the drug increases dramatically. To suppress the tumor at a larger tumor size with high proportion of resistance, theoretically, the effective dosage may exceed the maximum tolerance dosage (MTD). Under these situations, the elimination or the

complete cure may not be achieved, therefore, adaptive chemotherapy could be a better strategy for the patient to prolong the overall survival and improve life quality.

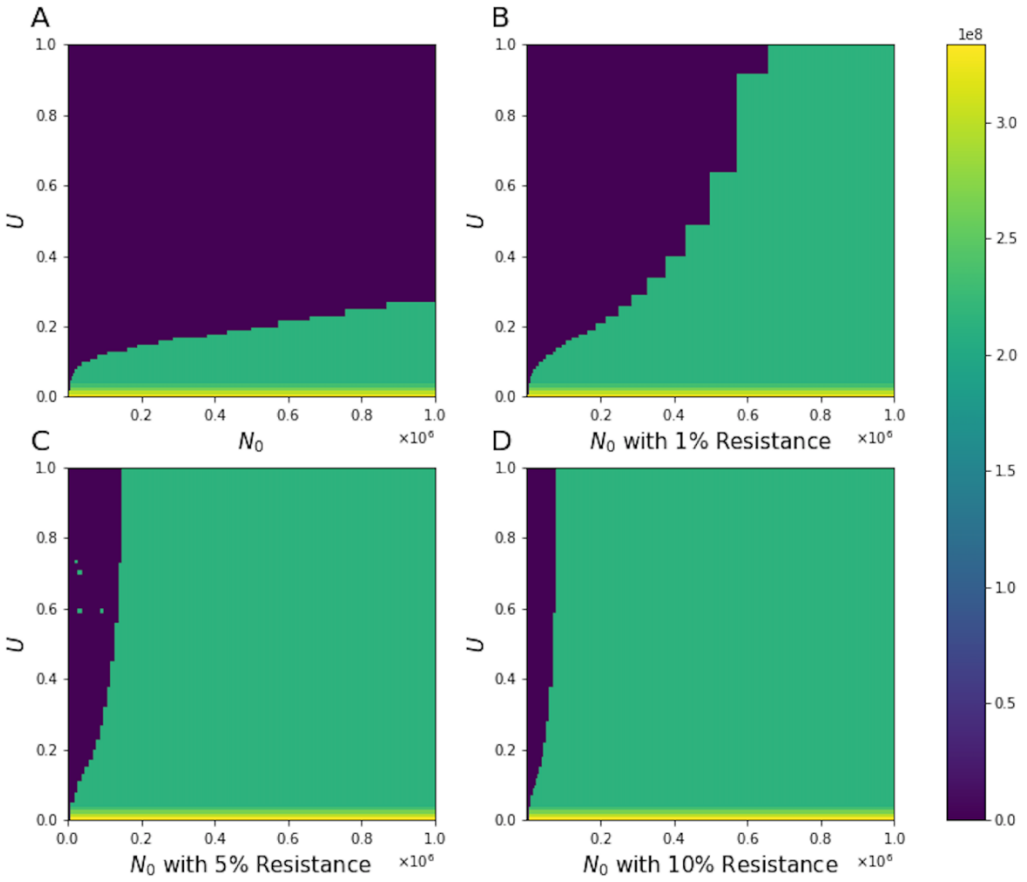

Figure 4-5 Tumor dynamics under multiple effective drug concentrations and initial tumor size

(A): No resistant phenotype, (B): 1% resistant phenotypes, (C):5% resistant phenotypes and (D):10% resistant phenotypes. The treatment starts with $\mathrm{A} = 10^3$. With an extremely low drug dosage, the wildtype dominates the tumor dynamics (yellow region); with the increase of the dosage, the resistant phenotype takes over the composition of the tumor cell population (green region); with sufficient dosage, the tumor cells could be eliminated, resulting in a complete cure of the cancer (dark blue region). The minimal drug dosage to complete cure increases as the tumor size and resistance composition initiated at treatment.

From these results, we observe a qualitatively difference in the treatment strategies resulting in different prognosis. The dynamics of our model framework is quite different than well-acknowledged logistic or Gompertzian models, which can be

approximate as exponential growth model at low cell densities. Compared with those traditional models containing two steady states 0 (unstable fixed point) and K (stable fixed point), our modification, introducing Allee threshold A, enables 0 and K steady states both to be stable. The various key factors, including tumor size, composition of resistant phenotypes, drug tolerance, together with Allee threshold determines the behavior of the system. Thus, at this stage, clinically, our model could explain the existence of the proportion of the patients living under tumor-free status after proper treatment protocols.

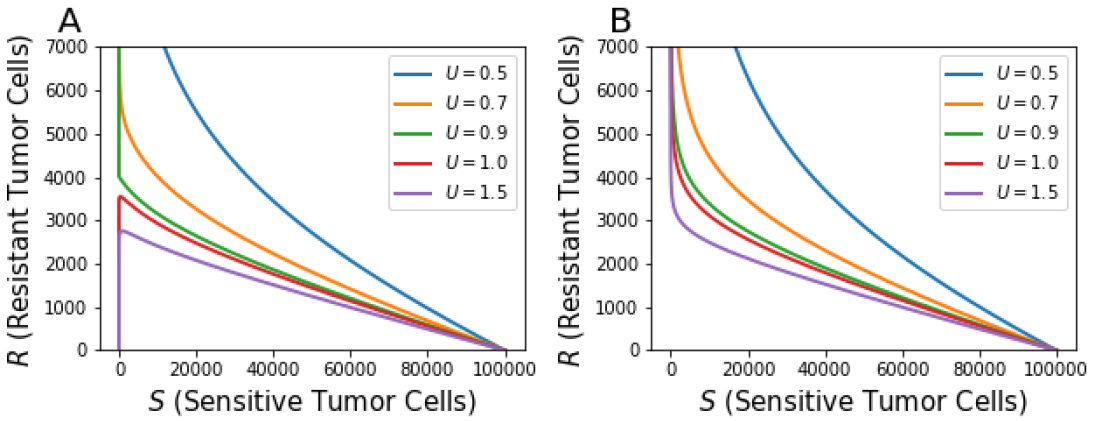

Figure 4-6 Tumor dynamics under multiple different growth models with constant dosage treatment

Initial condition: $S(0) = 10^5, R(0) = 0$ and $A = 10^3$. (A) Considering Allee effect, there exists a critical effective dosage between 0.9 and 1.0, above which the tumor can be eliminated. (B). Regardless of Allee effect, the tumor won't be eradicated, leaving the evolution towards drug resistant colonies, resulting in treatment failure, which suggests Allee effect is critical for the cure of the cancer.

4.5 Discussion

Recent preclinical and clinical observations of tumor initiation or recurrence indicates the presence of tumor growth kinetics positively scale with cell numbers indicating an Allee effect. In the current work, we established a tumor growth taking consideration of Allee effect. Using this model, we contrasted the effect of the dosage

for the treatment and demonstrate the different outcomes. Thus, understanding the dynamics of the tumor growth, evolution of the tumor and comprehensive evaluating tumor stages concerning to design effective therapy is crucial.

Brock et al confirmed the Allee effect in vitro at low cancer cell population, suggesting a more pronounced effect in vivo[39]. Allee threshold in our model, a comprehensive index, combines the immune response, nutrition level, tumor microenvironments and other key factors may limit the tumor growth at a low tumor cell density.

To demonstrate how the tumor stage and treatment protocols determine the prognosis theoretically, we performed analysis on effective chemotherapy dosage, initial tumor sizes, resistant cell compositions and Allee threshold: for a relatively lower tumor size and low proportion of resistant colonies, there exists a reasonable effective therapeutic dosage for tumor eradication. However, with the increase in drug resistance proportion and tumor size, the difficulty for eradication is increasing dramatically, leaving prolongation of tumor control a better strategy for cancer management. Also, with the increase of Allee threshold, a complex index in our model associated with in vivo status of the patient, the possibility of eradication is increasing accordingly.

4.5.1 Benefits of Combination Chemotherapy

Combination chemotherapy is a widely used strategy to lower the risk and delay the emergence of the resistant colonies. The drugs interactions, synergism could be more rapid in reducing the disease burden compared with single drug administration[26]; nonsynergistic drug combinations are more likely than synergistic combinations to

provide a long-term defense against the evolution of therapeutic resistance if these combinations have similar initial efficacy[86]. The combination of multiple drugs targeting distinct pathways brings the chance of cure far larger than apply them sequentially[20], this evolutionary dynamic model focusing on point mutations induced resistance offers valuable advice for the design of clinical trials. Our model further emphasizes the benefits of combination therapy in the dynamics at lower tumor cell densities, with the effect to lower the resistant proportion, where Fig 4.5 reveals this is the most effective and applicable way to increase the chance of tumor eradication.

4.5.2 Benefits of Adjuvant Chemotherapy

Adjuvant (additional) chemotherapy is an approach used after primary treatments, such as radical surgery, aiming to destroy the remaining but undetectable cancer cells and lower the recurrence chance. In this situation, based on our model's treatment protocol, the disease burden is typically no greater than detection threshold ($\sim 10^6$), therefore under a properly designed systematic adjuvant chemotherapy, according to the model prediction, the tumor could be eradicated. Combined with combination chemotherapy or proper chemotherapy agents in sequence, the chance of the tumor eradication could be increased.

4.5.3 Drug Strategies in Adjuvant or Progression-free Survival (PFS) Phase

Clinically, the detection of micro residual disease or remaining tumor cells is limited to certain threshold. Various mathematical models define PFS as the length of time where the total number of tumor cells is less than detection threshold as

$$T_{PFS} = \inf\{t: S + R \geq N_{Detect}\}.$$

This situation falls into our model's regime, where Allee effect together with drug resistance evolution play key roles in the cure of cancer, which is a great chance for tumor eradication. This period is like a black box of the treatment, where no clinical detection could be the evidence or the guidelines the personalized medication. Therefore, mathematical model is a powerful tool for inferring status of the patient and medication administration. A relatively intensive chemotherapy, combination chemotherapy and periodically switching of chemotherapy agents could be major strategies for a safe consolidation and lower the recurrence risks.

Our simple model allows significant insight into the roles of adjuvant chemotherapy and may help to explain how cancer cell populations are able to go extinct after therapy despite the prediction and may be promising to improve the predictions of tumor growth and relapse dynamics. More diligent models can be studied by incorporating more biological details.

5 Mathematical Framework of Combinational Chemotherapy Effects and the Evolution of Resistance

5.1 Abstract

One of the impediments of the successful cancer treatment is the development of drug resistance. Different regimens of chemotherapy may lead to different outcomes. Optimize chemotherapy regimens is critical in clinical practices. We propose a simple set of ordinary differential equations to quantify the effects of drug interactions: synergy, additive, and antagonism. The drug interactions lead to different evolutionary trajectories of phenotypic intratumor heterogeneity, thus resulting in different treatment outcomes. This framework suggests that synergy between drugs can efficiently reduce the tumor cell number (disease burden) in the short term but has the tradeoff of an earlier emergence of drug resistant. This conclusion is critical in designing combinational chemotherapy schedules and managing tumor progression of the patients.

5.2 Introduction

Cancer is an evolutionary disease, which exhibits striking heterogeneity[52,76], resulting in large variation in tumor initiation, progression, metastasis, therapeutic responses and recurrence[20,23,77,78]. Modern chemotherapy have impressive initial efficacy, however, the drug resistance often occurs during the treatment in a span of months[20,21,86] and become one of the major barriers for successful cure of the disease. Investigations on developing new efficient drugs and seeking for better combinations[26] and schedule[22,87,88] for administration of the chemo-agents are major strategies of improving cure rates and prolong patients' survival clinically. Various computational models are developed to predict the response of the treatments; optimal control methods are applied to the system to determine the dosing strategies and minimize the disease burden[89]; stochastic ordinary differential equations (SDEs) with pharmaceutical kinetics are applied to study the patients progression free survival (PFS) with combination targeted chemo-agents of melanoma patients[26] and ordinary differential equations (ODEs) systems could characterize the emergences of the drug resistance subclones of the tumor[21]. We here characterize the theoretical framework to study the combined effects of drugs and the influences on the treatment responses and outcomes.

When multiple drugs are used at the same time or in sequence, the interaction between the drugs can synergistic, additive, and antagonistic. Fig 5-1A shows the isobologram with equal efficacy for additive (diagonal line), synergistic (green region) and antagonistic (yellow region). Additive is characterized as the pair of the drugs act independently, therefore the overall effects of the drug pair is equal to the sum of

everyone. While the synergy has greater potency relative to the addition of each individual's efficacy, therefore seeking synergy effects of combinational agents are widely pursued in clinical settings[26,37]. Antagonism is less than additive effects, where one of the chemo-agents gives less benefits than mere usage of it alone, but it's still beneficial for the treatment. This is different from the antidote effect, where the usage of one drug cancels out the effects of other drugs.

In this work, we employ a non-spatial theoretical model framework to study the effects of a pair of drugs on the evolution of drug resistance in tumor cell population and the possible links to clinical practices.

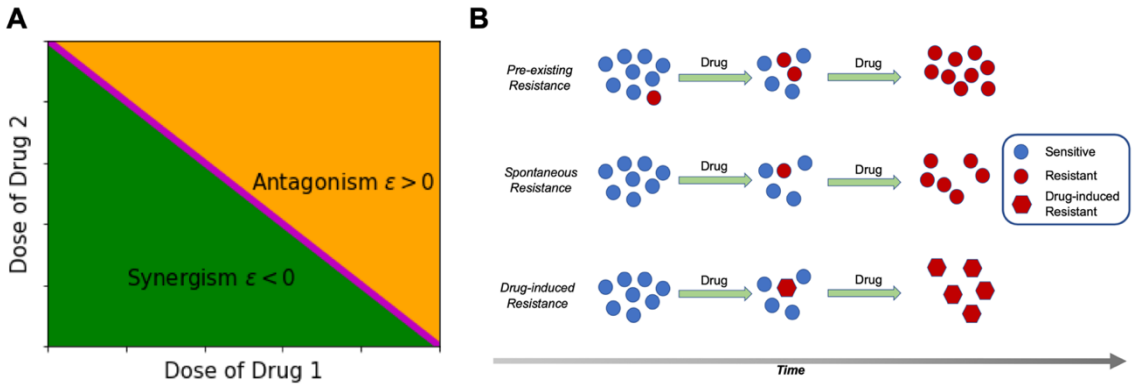

Figure 5-1 Schematic Diagram of Drug Interactions and Evolution of Multi-type Resistance during Chemotherapy

5.3 Methods

We consider a general mathematical framework to describe the synergism and antagonism effects of the combinational chemotherapy and the evolution of resistance. We consider the tumor composed of four phenotypes regards of the response to chemotherapy agents (Drug A and Drug B), sensitive (S), resistant only to drug A (R_A),

resistant only to drug B (R_B) and resistant to both (R_{AB}). Sensitive (wildtype) cells are fully susceptible to the treatment. We apply a system of ordinary differential equations to characterize the dynamics of the phenotypes and the evolution of drug resistance with all non-negative parameters:

$$D_{eff} = p_A D_A + p_B D_B + C D_A D_B \frac{p_A p_B}{ED_{50,2}} := p_A D_A + p_B D_B + C_{Com} D_A D_B p_A p_B$$

$$\dot{S} = rS\left(1 - \frac{S + R_A + R_B + R_{AB}}{K}\right) - SD_{eff} - (\alpha p_A D_A + \alpha p_B D_B + \epsilon_A + \epsilon_B)S$$

$$\dot{R_A} = \eta_A rS\left(1 - \frac{S + R_A + R_B + R_{AB}}{K}\right) - R_A p_B D_B + (\alpha p_A + \epsilon_A)S - (\alpha p_B + \epsilon_B)R_A$$

$$\dot{R_B} = \eta_B rS\left(1 - \frac{S + R_A + R_B + R_{AB}}{K}\right) - R_B p_A D_A + (\alpha p_B + \epsilon_B)S - (\alpha p_A + \epsilon_A)R_B$$

$$\dot{R_{AB}} = \eta_A \eta_B rS\left(1 - \frac{S + R_A + R_B + R_{AB}}{K}\right) + \alpha(p_A R_B + p_B R_A) + \epsilon_A R_B + \epsilon_B R_A$$

Table 5-1 Parameters for the Model Comparing Combination Chemotherapy Effects

Parameters	Biological Interpretation	Value (Range)	References
$S(t)$	**Sensitive Population**		
$R_A(t)$	**Resistant Population to Drug A**		
$R_B(t)$	**Resistant Population to Drug B**		
$R_{AB}(t)$	**Resistant Population to Both Drug A and B**		
r	**Net Proliferation Rate of the Tumor**	$0.01/Day$	(Bozic 2013)
$\eta_i(i = A, B)$	**Reduced Ratio of Growth Rate for Resistant**	$[0, 1]$	
$\alpha_i(i = A, B)$	**Drug-induced Resistance Rate**	$[10^{-5}, 10^{-1}]$	(Greene 2019)
$p_i(i = A, B)$	**Relative Drug Administration Dosing**	$[0, 1]$	
C_{Com}	**Drug Interaction Intensity**	$[-10^2, 10^2]$	(Saputra 2018)
$D_i(i = A, B)$	**Normalized Drug Efficacy at MTD**	10^{-2}	
K	**Carrying Capacity of Tumor**	10^{10}	(Xiaoqiang 2016)
$\epsilon_i(i = A, B)$	**Spontanous Mutation Rate for Drug Resistance**	$[10^{-6}, 10^{-5}]$	(Greene 2019)

5.3.1 The Effect of Combination Therapy

We adopted the Greco and colleagues' model[21,86] to characterize the effect of drug interactions: additive, synergism, and antagonism. We normalized the drug efficacy (D_i), reducing proliferation rate of the tumor, at maximum tolerated dose (MTD) for different chemotherapy agents for different phenotypes. We assume the efficacy of a certain agent is proportional to its dosing (p_i). If the drugs are independent and additive, the overall effects of the combination of the drug is a linear addition of the normalized drug efficacy ($D = \sum_i D_i\, p_i$), while if there're interactions among the drugs, the intensity of the combination effect is considered and illustrated in Figure 5-2. For our illustrative

model, without losing genericity, we only consider the combination of a pair of chemo agents.

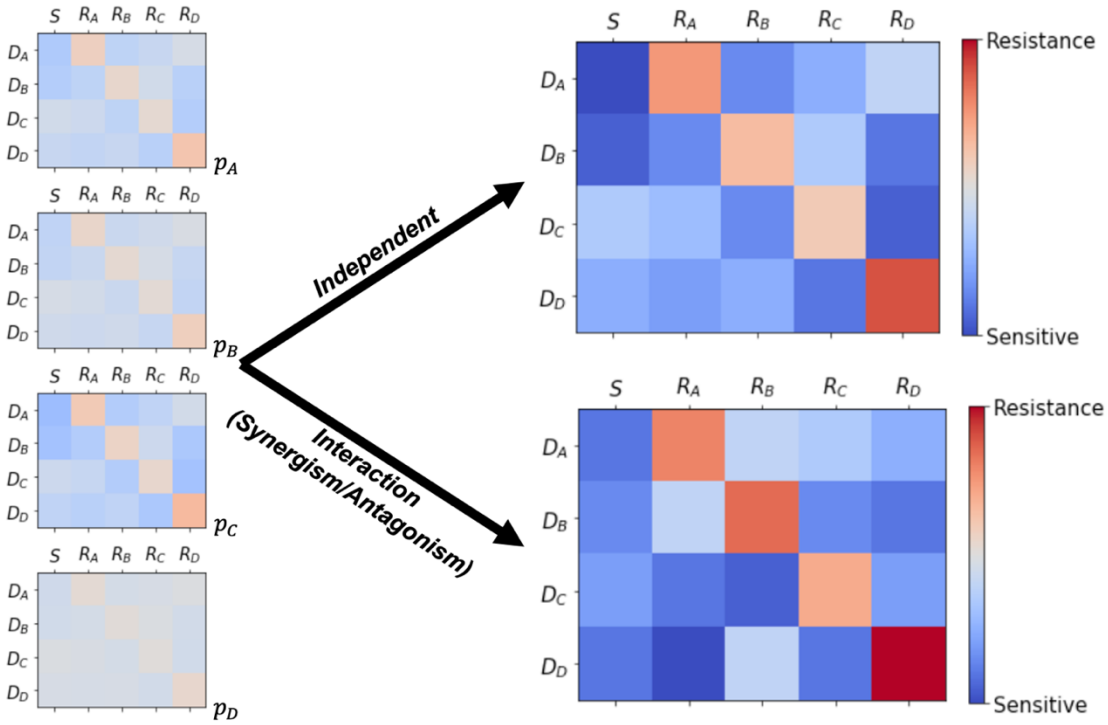

Figure 5-2 A Demo Drug Interaction (Synergy/Additive/Antagonism) Matrix
According to the sensitivity of the chemo-agents (blue for sensitive colony and red for the resistant), the tumor cells can be stratified as sensitive (S), resistant to certain drug (R_i). The dosage of the drug is p_i with a normalized drug efficacy D_i. The combination of the drug is simply additive if the drugs are independent (shown in the upper penal), while the more realistic setting is that the drugs have interactions, therefore the overall efficacy of the combinational chemotherapy is not simply additive.

5.3.2 Spontaneous and Drug-induced Resistance

Genetic, epigenetic, posttranslational mechanisms, cellular mechanisms, microenvironmental mechanisms and pharmacokinetic mechanisms[37] could result in resistance to the treatments. Mathematical models and experiments reveal, different drugs have different effects in inducing resistance[20,26], theoretical model using double-well potential explains the treatment intensity could reshape the tumor cells fitness[89].

The modeling of these complex mechanisms of the emergence of the resistance depends on the comprehension the procedures of the cellular-drug interactions, pharmaceutical kinetics, and many other biological details. Here, we adopt Greene's mathematical approach[21] to model the spontaneous (background mutations characterized by base mutation rates ϵ_i) and induced-resistance (dose-dependent characterized by α_i in the equations above).

5.4 Results

To quantify the effects of the evolution of drug resistance, the treatment protocol is specified here. We assume the disease is initiated and the treatment begins when all the cells are wild type:

$$S(0) = S_0 = 10^9, R(0) = 0$$

The administration of the drug is constant dosing. A progression free survival is defined as for comparison

$$T_{PFS} = \inf\{t: S + R \geq N_{Detect}\}.$$

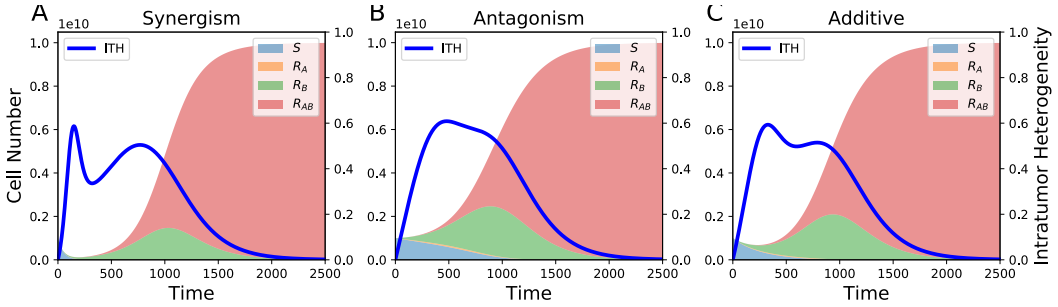

Figure 5-3 Evolution of Drug Resistance under Different Drug Interactions
(A). The disease burden is depicted in the shaded curve with the dominant sub colony (R_{AB}) of resistant to both drug A and B under the synergistic drug combination. The intratumoral heterogeneity (ITH) is shown in blue curve with two peaks under this chemotherapy regimen. (B). The dynamics of the tumor evolution under antagonism scenario. (C). The dynamics of the tumor evolution under no drug interactions scenario.

Fig 5-3 compares the drug resistance evolution under the scenario of drug synergism (A), additive (C) and antagonism (B). We define the phenotypic intratumor heterogeneity as

$$ITH := 1 - \sum_{i=1,\dots,n} \left(\frac{N_i}{N}\right)^2$$

The emergence of drug resistance leads to the treatment failure in all the situations (A, B, and C) in a long-term time scale: the resistance subclone R_{AB} to both drug A and B will become dominant.

The drug interactions lead to different evolutionary trajectories of phenotypic intratumor heterogeneity, thus resulting in different treatment outcomes. The drug synergy has the advantage to lower the disease burden initially. However, the resistance colony emergences and become dominate and lead to the treatment failure.

Figure 5-4(B) shows the progression free survival for drug synergy, when compared with no drug interactions, the PFS is a drawback for drug synergy treatment.

The drug antagonism reduces the effective efficacy in reducing the disease burden Fig 5-3 (B).

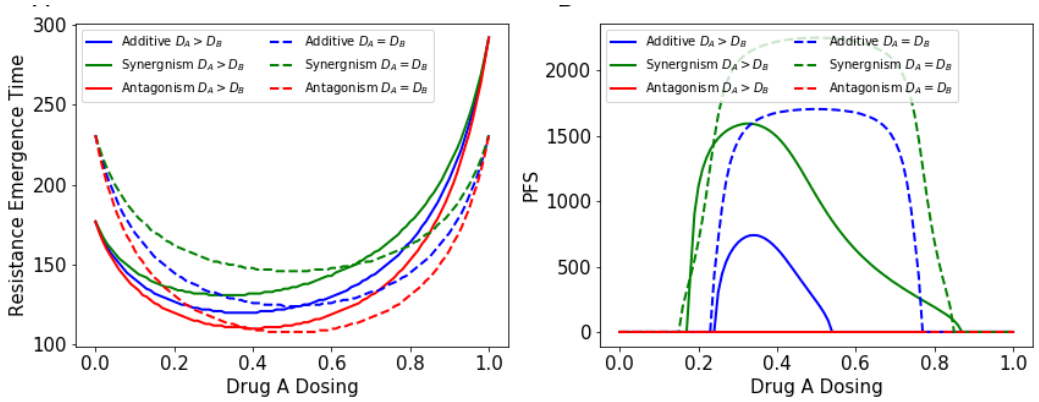

Figure 5-4 Emergence of Resistance and Progression Survival under Different Drug Interactions

This framework suggests the synergy effect, in short term, could efficiently reduce the tumor cell number (disease burden), but the trade-off, compared with antagonism drug combinations, is the earlier emergence of drug resistant subclones. This conclusion is essential and critical in designing combinational chemotherapy schedules and managing tumor progression of the patients.

6 CONCLUSIONS AND FUTURE WORK

6.1 Summary

Cancer is an evolutionary disease with genomic and phenotypic heterogeneity. This intratumor heterogeneity is one of the leading factors influencing the treatment responses, prognosis, and outcomes of patients in clinical practices. Two major reasons for treatment failure are metastasis and the emergence of chemo-resistance. Both metastasis and drug-resistance are direct consequences of the evolution of phenotypic ITH. The changing heterogeneity enables tumor cells to adapt to different selection pressure in different microenvironments, including those imposed by cancer treatments.

Cancer genomic heterogeneity has been extensively studied and helped to discover targeted chemo agents, stratification of high-risk patients, and benefitted patients in clinical practices. The phenotypical heterogeneity has not been as well understood. Our central goal is to understand the evolution of phenotypic heterogeneity as tumor cells adaptation to various environments. We use a multiscale model to systematically study cancer metastasis and make connections to potential clinical implications for optimizing screening and treatment schedules. At the cell level, we use a cell-based model (the Cellular Potts Model or CPM) to simulate the collective cancer invasion. At the population level, we use continuous replicator dynamics to analysis the adaptation strategies of the tumor.

Collective cancer invasion, where cells invade into peritumoral stroma as a cohesive and polarized mass maintaining cell-cell contacts, is shown to associate with better metastatic success and poor patient outcome. Even though we have identified distinct phenotypes in the collective invasion pack, the interactions between the

phenotypes and between cells and the microenvironment have not been well understood. The experiments distinguished leader cells and follower cells in both behaviors and genomic differences[23,27,31] and confirms the existence of at least two distinct phenotypes. Then we introduce a Cellular Potts Model (CPM) to establish a framework to depict the phenomena emerged in collective cancer invasion spheroids for non-small cell lung cancer cell line in vitro. This framework can serve as a testbed to incorporate the biological details, such as pairwise interactions between leader cells and follower cells[31], interaction with extracellular matrix[35,40–42] and etc.

In chapter 3, We use a game theory framework to decipher the roles of pairwise interactions in leader-follower collective invasion and analyze the dynamics of the system under various interaction intensities. These results suggest novel targets or treatment strategies to reduce tumor burden as well as lower metastatic risks.

Besides the metastasis, another major reason causing treatment failure of cancer is drug resistance. We apply continuous model to explore the tumor growth dynamics and drug resistance evolution. Therefore, s better understanding of the tumor cell growth is needed. The dynamics of tumor growth are extensively studied for decades[43–46]. In chapter 4, we re-examine the tumor growth at low cell density because recent experiments which examine the tumor cell population at low cell density reveal the growth dynamic deviate from exponential growth pattern and indicate an Allee effect in vitro[39]. This effect is expected to be much stronger in vivo[39] and could result in significant understanding of tumor progression. Here, we incorporate this ecological principle in our tumor growth model along with drug resistance to control tumor progression and eradication. Our model reveals the relationships between tumor size

(disease burden), intratumor heterogeneity in terms of drug sensitivity, treatment dosage, and the probability of tumor eradication. These results offer more optimal therapeutic strategies based on personalized treatment goals.

In chapter 5, the usage of combinational chemotherapy and drug interactions are discussed. The seeking for optimal chemotherapy regimens is critical in clinical practices, the optimal choices of a combinational chemotherapy agents and proper administration could result in different outcome for the patients. We propose a simple set of ordinary differential equations to quantify the effects of drug interactions: synergy, additive and antagonism. The drug interactions lead to different evolutionary trajectories of phenotypic intratumor heterogeneity (ITH), thus resulting in different treatment outcomes. This framework suggests the synergy effect, in short term, could efficiently reduce the tumor cell number (disease burden), but the trade-off, compared with antagonism drug combinations, is the earlier emergence of drug resistant subclones. This conclusion is essential and critical in designing combinational chemotherapy schedules and managing tumor progression of the patients.

This work reveals how the pairwise interactions between phenotypes within the tumor, together with the microenvironments, alter the dynamics of the tumor progression and change their responses to chemotherapy. The study will offer potential clinical prognosis information and treatment strategies for patients.

6.2 Future Work

Cancer is an evolutionary disease which exhibits striking genomic and phenotypic intratumor heterogeneity. Our understanding of the cancer progression and evolution is also evolving. In this dissertation, we apply agent-based model, evolutionary game theory and continuous models to study the evolution of phenotypic intratumor heterogeneity in terms of drug sensitivity and metastasis.

One of the next directions is to embed the evolutionary game theory to agent-based model to explore the evolution of phenotypic intratumor heterogeneity with spatial information. An intermediate state can be added to the framework to explore the influences in collective cancer invasion process. Meanwhile, leader and follower cells and their pairwise interactions[23,27,31], role of extracellular matrix[35,40,54] and a variety of detailed biological factors can be embedded in the model to enrich the dynamics of the mathematical models.

1. Pairwise interactions: recent experiments using SaGA, a fluorescent imaging technique, observe leader and follower behaviors in NSCLC spheroids in vitro[23,27]. These two distinct phenotypes exchange signaling molecules[31] to coordinates leader-follower behaviors in collective invasion. The leader provides escaping mechanism for the followers and follower cells can secrete an undefined proliferation signal to promote the growth of leader cells, confirmed by experiment observation that the follower-only media increases leader cells proliferation rate[23]. Leader cells secrete VEGF, which is taken up by follower cells and results in follower cells to follower them. However, the leader cells can secrete a growth

inhibitor that reduces the proliferation rate of the follower cells. These complex pairwise interactions could enrich the dynamics of leader-follower behaviors in collective invasion, which can be incorporated to this agent-based model framework.

2. Other biological factors: Another direction might be to modify this model framework with more detailed biological factors, such as interactions with extracellular matrix, stroma, immune system etc. Other than these pairwise interactions mentioned above, fibronectin, one of the important biological molecules forming extracellular matrix[72], secretion by leader cells can expand the leader cells' domain, therefore relax the competition pression on leader cells proliferation[31]. Ordinary differential equations model predicts that when altering the signaling environment, the relationship of the cell types and the development of the complex system can be altered[31]. We can embed the extracellular matrix (mainly fibronectin) in the framework and explore the dynamics of the collective invasion with spatial information. This information is crucial and will enrich our understanding towards collective cancer invasion may shed light on potential applications in clinical settings, such as diagnosis, novel target chemo-agents preventing metastasis etc.

Another next future research direction is to seek link between the model and preclinical or clinical data. We can fit the model to some preclinical or clinical date to better guide the potential treatment and have a more comprehensive and evolving understanding of cancer. In chapter 4, we re-examine the tumor growth at low cell

density because recent experiments which examine the tumor cell population at low cell density reveal the growth dynamic deviate from exponential growth pattern and indicate an Allee effect in vitro[39]. This effect is expected to be much stronger in vivo[39] and could result in significant understanding of tumor progression. This model uses an Allee threshold (A) to embed the possible complex biological factors which could result in the deviations from tumor exponential growth at low cell density. The validation of the model is critical and could shine light upon the clinical cancer treatments.

1. To find the Allee effect requires the observation of cancer at low cell density, which is not always possible during clinical trials and difficult to obtain data in vivo. Furthermore, this effect can be masked by other factors such as immune responses, drug efficacy, heterogeneity of cell growth rate and other factors. However, in this model, we see a divergence between tumor eradication and co-evolution with tumor in vivo, the recurrence time and rate of the cancer can serve as the indicator data to validate the model. Delitala et al apply an Allee growth model to fit the tumor burden of colon-rectal cancer[90]. Therefore, we can estimate the order of Allee threshold in a given type of cancer in vivo.
2. The recurrence of cancer is one of the major impediments to cure cancer. The patients typically go to remission status after first-round effective treatments, during which the cancer cells cannot be detected. However, some of the tumors relapse after several months or even years, therefore, developing effective management strategies at disease-free state for higher recurrence rate patients is essential. This model could illustrate the dynamics

of the tumor cells at low cell density and provide insights to prevent the recurrence.

Cancer is a dynamic complex multi-scale system that can only truly be better understood via integration of theories and experiments. Tumor is heterogeneous which exhibits striking genomic and phenotypic heterogeneity. When sampling a tumor, it is common to see different types of cancer cells with different morphology, antigen expressions and other properties. The advent of sequencing technique enables the researchers and clinicians to see the composition of the tumor and have a comprehensive understanding of the tumor evolution traces. Therefore, they can better understand the interactions between different phenotypes and the emergence of some phenotypes. In this dissertation, we analysis the dynamics of the phenotypical ITH in the process of collective invasion and treatments under different regimens of chemotherapy. The study is to understand the evolution of phenotypical ITH, a characterization indicates the tumor's adaptation to different environments or selection pressures.

REFERENCES

1. Wang, H. *et al.* Global, regional, and national life expectancy, all-cause mortality, and cause-specific mortality for 249 causes of death, 1980–2015: a systematic analysis for the Global Burden of Disease Study 2015. *Lancet* **388**, 1459–1544 (2016).
2. Hanahan, D. & Weinberg, R. A. Hallmarks of cancer: The next generation. *Cell* **144**, 646–674 (2011).
3. Hanahan, D. & Weinberg, R. A. The Hallmarks of Cancer. *Cell* **100**, 57–70 (2000).
4. Stout, I. J. & Odum, E. P. Fundamentals of Ecology. *J. Wildl. Manage.* **36**, 1372 (1972).
5. Merlo, L. M. F., Pepper, J. W., Reid, B. J. & Maley, C. C. Cancer as an evolutionary and ecological process. *Nat. Rev. Cancer* **6**, 924–935 (2006).
6. Korolev, K. S., Xavier, J. B. & Gore, J. Turning ecology and evolution against cancer. *Nat. Rev. Cancer* **14**, 371–380 (2014).
7. Beerenwinkel, N., Schwarz, R. F., Gerstung, M. & Markowetz, F. Cancer evolution: Mathematical models and computational inference. *Syst. Biol.* **64**, e1–e25 (2015).
8. Nowak, M. A. *Evolutionary Dynamics: Exploring the Equations of Life*. *Belknap Press of Harvard University Press,* (Belknap Press of Harvard University Press, 2006).
9. Pacheco, J. M., Santos, F. C. & Dingli, D. The ecology of cancer from an evolutionary game theory perspective. *Interface Focus* **4**, (2014).
10. West, J., Hasnain, Z., Mason, J. & Newton, P. K. The prisoner's dilemma as a

cancer model. *Converg. Sci. Phys. Oncol.* **2**, 035002 (2016).

11. Hummert, S. *et al.* Evolutionary game theory: Cells as players. *Mol. Biosyst.* **10**, 3044–3065 (2014).
12. Davis, A., Gao, R. & Navin, N. Tumor evolution: Linear, branching, neutral or punctuated? *Biochim. Biophys. Acta - Rev. Cancer* **1867**, 151–161 (2017).
13. Fittall, M. W. & Van Loo, P. Translating insights into tumor evolution to clinical practice: Promises and challenges. *Genome Med.* **11**, 1–14 (2019).
14. Cannataro, V. L. *et al.* Heterogeneity and mutation in KRAS and associated oncogenes: Evaluating the potential for the evolution of resistance to targeting of KRAS G12C. *Oncogene* **37**, 2444–2455 (2018).
15. Somarelli, J. A. *et al.* Molecular Biology and Evolution of Cancer: From Discovery to Action. *Mol. Biol. Evol.* **37**, 320–326 (2020).
16. Gatenby, R. A., Silva, A. S., Gillies, R. J. & Frieden, B. R. Adaptive therapy. *Cancer Res.* **69**, 4894–4903 (2009).
17. Zhao, B., Hemann, M. T. & Lauffenburger, D. A. Intratumor heterogeneity alters most effective drugs in designed combinations. *Proc. Natl. Acad. Sci. U. S. A.* **111**, 10773–10778 (2014).
18. Rockne, R. C. *et al.* The 2019 mathematical oncology roadmap. *Phys. Biol.* **16**, (2019).
19. Wodarz, D. & Komarova, N. *Computational Biology of Cancer*. *Computational Biology of Cancer* (2005). doi:10.1142/5642.
20. Bozic, I. *et al.* Evolutionary dynamics of cancer in response to targeted combination therapy. *Elife* **2013**, 1–15 (2013).

21. Greene, J. M., Gevertz, J. L. & Sontag, E. D. Mathematical Approach to Differentiate Spontaneous and Induced Evolution to Drug Resistance During Cancer Treatment. *JCO Clin. Cancer Informatics* 1–20 (2019) doi:10.1200/cci.18.00087.

22. Yoon, N., Vander Velde, R., Marusyk, A. & Scott, J. G. *Optimal Therapy Scheduling Based on a Pair of Collaterally Sensitive Drugs*. *Bulletin of Mathematical Biology* vol. 80 (Springer US, 2018).

23. Konen, J. *et al.* Image-guided genomics of phenotypically heterogeneous populations reveals vascular signalling during symbiotic collective cancer invasion. *Nat. Commun.* **8**, 1–15 (2017).

24. Seguin, L., Desgrosellier, J. S., Weis, S. M. & Cheresh, D. A. Integrins and cancer: Regulators of cancer stemness, metastasis, and drug resistance. *Trends Cell Biol.* **25**, 234–240 (2015).

25. Wang, X., Zhang, H. & Chen, X. Drug resistance and combating drug resistance in cancer. *Cancer Drug Resist.* (2019) doi:10.20517/cdr.2019.10.

26. Sun, X., Bao, J. & Shao, Y. Mathematical Modeling of Therapy-induced Cancer Drug Resistance: Connecting Cancer Mechanisms to Population Survival Rates. *Sci. Rep.* **6**, 1–12 (2016).

27. Zoeller, E. L. *et al.* Genetic heterogeneity within collective invasion packs drives leader and follower cell phenotypes. *J. Cell Sci.* **132**, (2019).

28. Basanta, D., Hatzikirou, H. & Deutsch, A. Studying the emergence of invasiveness in tumours using game theory. *Eur. Phys. J. B* **63**, 393–397 (2008).

29. Liang, Y., Mcdonnell, S. & Clynes, M. Liang Y, McDonnell S, Clynes MExamining

the relationship between cancer invasion/metastasis and drug resistance. Curr Cancer Drug Targets 2:257-277. *Curr. Cancer Drug Targets* **2**, 257–277 (2002).

30. Mehta, K., Fok, J., Miller, F. R., Koul, D. & Sahin, A. A. Prognostic significance of tissue transglutaminase in drug resistant and metastatic breast cancer. *Clin. Cancer Res.* **10**, 8068–8076 (2004).
31. Haney, S., Konen, J., Marcus, A. I. & Bazhenov, M. The complex ecosystem in non small cell lung cancer invasion. *PLoS Comput. Biol.* **14**, 1–21 (2018).
32. Szabó, A. & Merks, R. M. H. Cellular Potts modeling of tumor growth, tumor invasion, and tumor evolution. *Front. Oncol.* **3 APR**, 1–12 (2013).
33. Graner, F. & Glazier, J. A. Simulation of biological cell sorting using a two-dimensional extended Potts model. *Phys. Rev. Lett.* **69**, 2013–2016 (1992).
34. Boareto, M., Jolly, M. K., Ben-Jacob, E. & Onuchic, J. N. Jagged mediates differences in normal and tumor angiogenesis by affecting tip-stalk fate decision. *Proc. Natl. Acad. Sci. U. S. A.* **112**, E3836–E3844 (2015).
35. Kumar, S., Kapoor, A., Desai, S., Inamdar, M. M. & Sen, S. Proteolytic and non-proteolytic regulation of collective cell invasion: Tuning by ECM density and organization. *Sci. Rep.* **6**, 1–17 (2016).
36. Hou, Y., Konen, J., Brat, D. J., Marcus, A. I. & Cooper, L. A. D. TASI: A software tool for spatial-temporal quantification of tumor spheroid dynamics. *Sci. Rep.* **8**, 1–9 (2018).
37. Sun, X. & Hu, B. Mathematical modeling and computational prediction of cancer drug resistance. *Brief. Bioinform.* **19**, 1382–1399 (2017).
38. Yin, A., Moes, D. J. A. R., van Hasselt, J. G. C., Swen, J. J. & Guchelaar, H. J. A

Review of Mathematical Models for Tumor Dynamics and Treatment Resistance Evolution of Solid Tumors. *CPT Pharmacometrics Syst. Pharmacol.* **8**, 720–737 (2019).

39. Johnson, K. E. *et al.* Cancer cell population growth kinetics at low densities deviate from the exponential growth model and suggest an Allee effect. *PLOS Biol.* **17**, e3000399 (2019).
40. Nguyen Edalgo, Y. T., Zornes, A. L. & Ford Versypt, A. N. A hybrid discrete–continuous model of metastatic cancer cell migration through a remodeling extracellular matrix. *AIChE J.* **65**, 1–15 (2019).
41. Triulzi, T. *et al.* Neoplastic and Stromal Cells Contribute to an Extracellular Matrix Gene Expression Profile Defining a Breast Cancer Subtype Likely to Progress. *PLoS One* **8**, 1–10 (2013).
42. Edalgo, Y. T. N. & Versypt, A. N. F. Mathematical modeling of metastatic cancer migration through a remodeling extracellular matrix. *Processes* **6**, 1–16 (2018).
43. Norton, L. A Gompertzian Model of Human Breast Cancer Growth. *Cancer Res.* **48**, 7067–7071 (1988).
44. Gerlee, P. The model muddle: In search of tumor growth laws. *Cancer Res.* **73**, 2407–2411 (2013).
45. González, M. M. *et al.* Is cancer a pure growth curve or does it follow a kinetics of dynamical structural transformation? *BMC Cancer* **17**, 1–14 (2017).
46. Westy, J., Hasnainy, Z., Macklinz, P. & Newtonyx, P. K. An evolutionary model of tumor cell kinetics and the emergence of molecular heterogeneity driving gompertzian growth. *SIAM Rev.* **58**, 716–736 (2016).

47. Molina, J. R., Yang, P., Cassivi, S. D., Schild, S. E. & Adjei, A. A. Non-small cell lung cancer: Epidemiology, risk factors, treatment, and survivorship. *Mayo Clin. Proc.* **83**, 584–594 (2008).

48. Greaves, M. & Maley, C. C. Clonal evolution in cancer. *Nature* **481**, 306–313 (2012).

49. Korolev, K. S., Xavier, J. B. & Gore, J. Turning ecology and evolution against cancer. *Nat. Rev. Cancer* **14**, 371–380 (2014).

50. Nam, A. *et al.* Suppressing chemoresistance in lung cancer via dynamic phenotypic switching and intermittent therapy. (2020) doi:10.1101/2020.04.06.028472.

51. Tan, B. L. & Norhaizan, M. E. Curcumin combination chemotherapy: The implication and efficacy in cancer. *Molecules* **24**, 1–21 (2019).

52. Gerlinger, M. *et al.* Intratumor heterogeneity and branched evolution revealed by multiregion sequencing. *N. Engl. J. Med.* **366**, 883–892 (2012).

53. Swat, M. H. *et al.* Modeling of Tissues Using CompuCell3D Methods. 325–366 (2012) doi:10.1016/B978-0-12-388403-9.00013-8.Multi-Scale.

54. Izaguirre, J. A. *et al.* CompuCell, a multi-model framework for simulation of morphogenesis. *Bioinformatics* **20**, 1129–1137 (2004).

55. Camley, B. A. & Rappel, W. J. Physical models of collective cell motility: From cell to tissue. *J. Phys. D. Appl. Phys.* **50**, (2017).

56. Barton, D. L., Henkes, S., Weijer, C. J. & Sknepnek, R. *Active Vertex Model for cell-resolution description of epithelial tissue mechanics*. *PLoS Computational Biology* vol. 13 (2017).

57. Van Liedekerke, P., Palm, M. M., Jagiella, N. & Drasdo, D. *Simulating tissue mechanics with agent-based models: concepts, perspectives and some novel results*. *Computational Particle Mechanics* vol. 2 (Springer International Publishing, 2015).

58. Metzcar, J., Wang, Y., Heiland, R. & Macklin, P. A Review of Cell-Based Computational Modeling in Cancer Biology. *JCO Clin. Cancer Informatics* 1–13 (2019) doi:10.1200/cci.18.00069.

59. Li, J. F. & Lowengrub, J. The effects of cell compressibility, motility and contact inhibition on the growth of tumor cell clusters using the Cellular Potts Model. *J. Theor. Biol.* **343**, 79–91 (2014).

60. Masuzzo, P., Van Troys, M., Ampe, C. & Martens, L. Taking Aim at Moving Targets in Computational Cell Migration. *Trends Cell Biol.* **26**, 88–110 (2016).

61. Winner, K. R. K. *et al.* Spatial modeling of drug delivery routes for treatment of disseminated ovarian cancer. *Cancer Res.* **76**, 1320–1334 (2016).

62. Gorochowski, T. E. Agent-based modelling in synthetic biology. *Essays Biochem.* **60**, 325–336 (2016).

63. Brodland, G. W. How computational models can help unlock biological systems. *Semin. Cell Dev. Biol.* **47**–**48**, 62–73 (2015).

64. Böttger, K. *et al.* An Emerging Allee Effect Is Critical for Tumor Initiation and Persistence. *PLoS Comput. Biol.* **11**, 1–14 (2015).

65. Neufeld, Z. *et al.* The role of Allee effect in modelling post resection recurrence of glioblastoma. *PLoS Comput. Biol.* **13**, 1–14 (2017).

66. Sewalt, L., Harley, K., van Heijster, P. & Balasuriya, S. Influences of Allee effects

in the spreading of malignant tumours. *J. Theor. Biol.* **394**, 77–92 (2016).

67. Szczurek, E., Krueger, T., Klink, B. & Beerenwinkel, N. a Stochastic Model of Metastatic Bottleneck. *Bioarxiv* (2018).
68. Bauer, A. L., Jackson, T. L. & Jiang, Y. A cell-based model exhibiting branching and anastomosis during tumor-induced angiogenesis. *Biophys. J.* **92**, 3105–3121 (2007).
69. Boareto, M. *et al.* Notch-Jagged signalling can give rise to clusters of cells exhibiting a hybrid epithelial/mesenchymal phenotype. *J. R. Soc. Interface* **13**, (2016).
70. Boareto, M. *et al.* Jagged-delta asymmetry in Notch signaling can give rise to a sender/receiver hybrid phenotype. *Proc. Natl. Acad. Sci. U. S. A.* **112**, E402–E409 (2015).
71. Clewley, R. Hybrid Models and Biological Model Reduction with PyDSTool. *PLoS Comput. Biol.* **8**, (2012).
72. Pankov, R. & Yamada, K. M. Fibronectin at a glance. *J. Cell Sci.* **115**, 3861–3863 (2002).
73. Böttcher, M. A. *et al.* Modeling treatment-dependent glioma growth including a dormant tumor cell subpopulation. *BMC Cancer* **18**, 1–12 (2018).
74. Kumar, N. *et al.* Stochastic modeling of phenotypic switching and chemoresistance in cancer cell populations. *Sci. Rep.* **9**, 1–10 (2019).
75. Nam, A., Mohanty, A., Bhattacharya, S., Kotnala, S. & Achuthan, S. Suppressing chemoresistance in lung cancer via dynamic phenotypic switching and intermittent therapy. (2020).

76. Mahdipour-Shirayeh, A., Kaveh, K., Kohandel, M. & Sivaloganathan, S. Phenotypic heterogeneity in modeling cancer evolution. *PLoS One* **12**, 1–27 (2017).

77. Lim, S. Bin *et al.* Addressing cellular heterogeneity in tumor and circulation for refined prognostication. *Proc. Natl. Acad. Sci. U. S. A.* **116**, 17957–17962 (2019).

78. Stanta, G. & Bonin, S. Overview on clinical relevance of intra-tumor heterogeneity. *Front. Med.* **5**, 1–10 (2018).

79. Courchamp, F., Berec, L. & Gascoigne, J. Allee Effects in Ecology and Conservation. *Allee Eff. Ecol. Conserv.* 1–272 (2008) doi:10.1093/acprof:oso/9780198570301.001.0001.

80. Stephens, P. A. & Sutherland, W. J. Consequences of the Allee effect for behaviour, ecology and conservation. *Trends Ecol. Evol.* **14**, 401–405 (1999).

81. Johnson, K. E. *et al.* Cancer cell population growth kinetics at low densities deviate from the exponential growth model and suggest an Allee effect. *PLoS Biol.* **17**, 1–29 (2019).

82. Panigrahy, D. *et al.* Epoxyeicosanoids stimulate multiorgan metastasis and tumor dormancy escape in mice. *J. Clin. Invest.* **122**, 178–191 (2012).

83. Simon, R. & Norton, L. The Norton - Simon hypothesis: Designing more effective and less toxic chemotherapeutic regimens. *Nat. Clin. Pract. Oncol.* **3**, 406–407 (2006).

84. Scholl, S. M. *et al.* Breast tumour response to primary chemotherapy predicts local and distant control as well as survival. *Eur. J. Cancer* **31**, 1969–1975 (1995).

85. Donadieu, J. & Hill, C. Early response to chemotherapy as a prognostic factor in

childhood acute lymphoblastic leukaemia: A methodological review. *Br. J. Haematol.* **115**, 34–45 (2001).

86. Saputra, E. C., Huang, L., Chen, Y. & Tucker-Kellogg, L. Combination therapy and the evolution of resistance: The theoretical merits of synergism and antagonism in cancer. *Cancer Res.* **78**, 2419–2431 (2018).
87. Yoon, N., Krishnan, N. & Scott, J. Modeling collaterally sensitive drug cycles: shaping heterogeneity to allow adaptive therapy. (2020) doi:10.1101/2020.07.02.184952.
88. Vander Velde, R. *et al.* Resistance to targeted therapies as a multifactorial, gradual adaptation to inhibitor specific selective pressures. *Nat. Commun.* **11**, (2020).
89. Akhmetzhanov, A. R. *et al.* Modelling bistable tumour population dynamics to design effective treatment strategies. *J. Theor. Biol.* **474**, 88–102 (2019).
90. Delitala, M. & Ferraro, M. Is the allee effect relevant in cancer evolution and therapy? *AIMS Math.* **5**, 7649–7660 (2020).